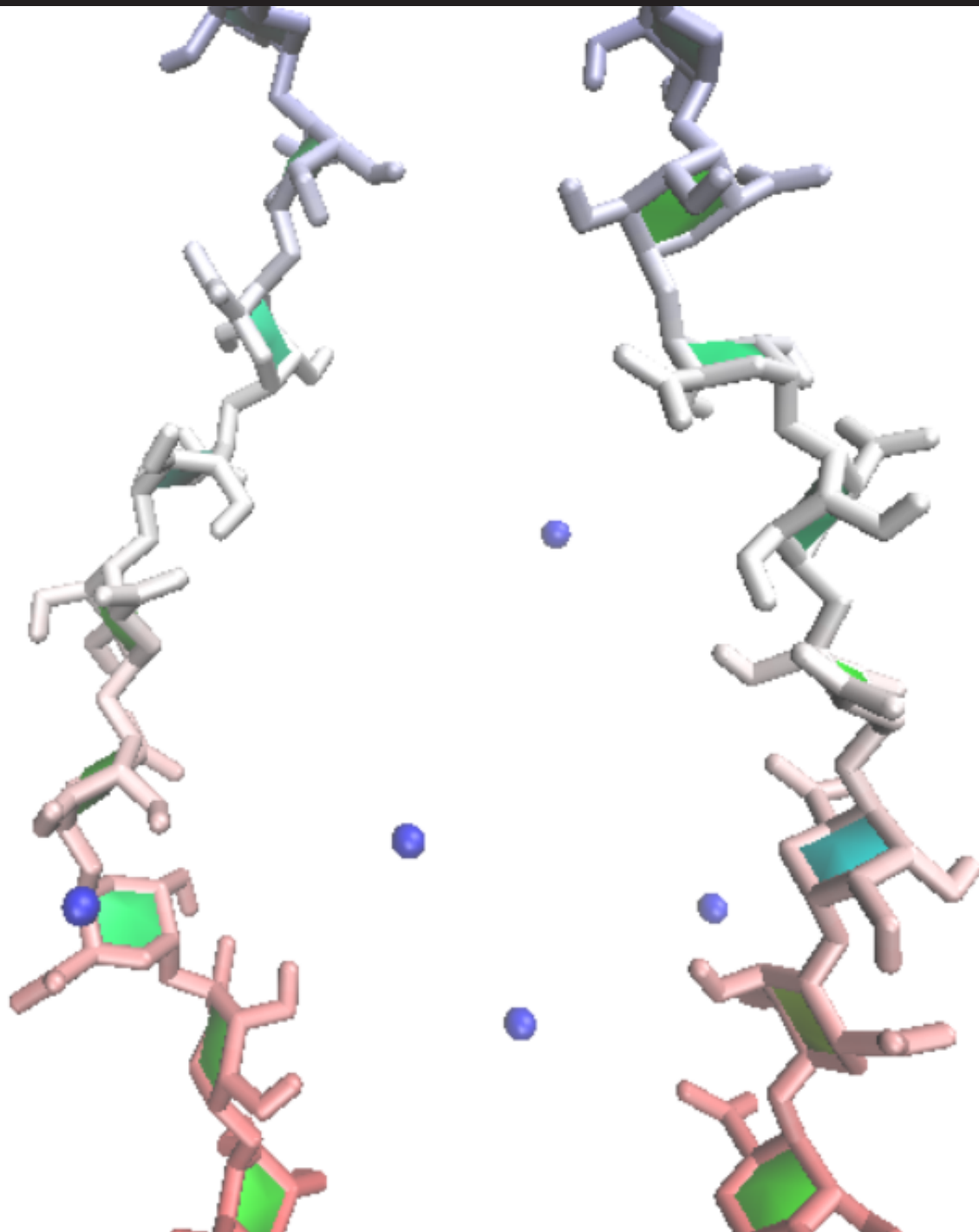


# Feasibility Study of Alginate Polymer Electrolytes through Molecular Dynamics Simulations

Santhosh Shetty

Technische Universiteit Delft





# Feasibility Study of Alginate Polymer Electrolytes through Molecular Dynamics Simulations

**Santhosh Shetty**

**Master of Science**

in Sustainable Energy Technology

Electrochemical Energy Storage  
Department of Radiation Science & Technology  
Faculty of Applied Sciences  
Delft University of Technology

to be defended publicly on Tuesday July 17, 2018 at 03:00 PM.

Supervisor : Dr. E. Kelder  
Thesis Committee : Dr. S. Picken  
Dr. E. Kelder  
Dr. M. Wagemaker  
Daily Supervisor : Dr. S. Basak

*This thesis is confidential and cannot be made public until December 31, 2018.*

An electronic version of this thesis is available at <http://repository.tudelft.nl/>.

# Abstract

Large scale stationary energy storage is becoming the need of the hour as the world transitions to a renewable economy. For this, there is a necessity of higher energy density batteries that can cope well both in storing excess energy and minimizing fluctuations on the grid. Solid polymer electrolyte batteries can be extremely safe and reduce packaging while also preventing dendrite formation in Lithium-ion batteries.

Sodium ion movement is seen from one oxygen atom to another for an arbitrary  $Na^+$  ion. This thesis shows that MD simulations can be a promising method to study the mechanisms involved in alginate polymer electrolytes. Further work is necessary to enable rigorous analysis by incorporating both mannuronates and guluronates. Neutron Magnetic Resonance (NMR) can be carried out to validate the results obtained through MD simulations.

MD simulations on sodium alginate (primarily of guluronate) as a solid polymer electrolyte appear to indicate the interaction of  $Na^+$  ion with  $O2$  atom of the polyguluronate residue is in preference to interaction of  $Na^+$  ion with carboxylate oxygen atoms. Diffusion constant of  $Na^+$  ion is seen to drop in MD simulations with increase in  $Ca^{2+}$  ion concentrations both at temperatures 300 K and 373 K.

**Keywords:** solid polymer electrolyte; molecular dynamics; interaction energy; diffusion constant; alginate.

# Acknowledgment

When I first set out to take up this thesis, I wanted to develop something that could help solve problems associated with the Lithium-Sulfur battery as it has a much higher energy density and can contribute to stationary energy storage which is in dire need today. It also made sense to work on the one which could be one of the first of next in line to Lithium-ion batteries. My work pivoted and I eventually ended up researching simulation techniques for understanding solid polymer electrolytes which could be one of the potential problem solvers for Lithium-Sulfur batteries. I am deeply thankful for Dr. Erik Kelder for giving me the opportunity to work on something that I am passionate about. I also cherish the insightful discussions that we had during which I learned a lot.

My daily supervisor, Dr. Shibabrata Basak was instrumental in charting out my process throughout my entire Master thesis period. When things didn't work or weren't explainable, he was always there to provide advice and guidance on what needed to be done. I am grateful for his constant support.

This project could not have been possible without the immense support of Mr. Jouke Heringa whose knowledge in conducting the simulations I found impressive. I am extremely grateful for his efforts and for his patience with me.

It was wonderful to have Mr. Frans Ooms as our lab technician. His love towards work is contagious. Despite being a busy man, Mr. Frans loves to help students with their doubts. I could approach him with any doubt and he knew the answers to all things related to batteries. For this, I am incredibly grateful.

I am lucky to have great friends whose camaraderie during my entire Master's period has been helpful and wonderful. Alex, Manoj, Abhilash, Praveen, Nikhil, Shreyas, Ajay and Anshul have been constant sources of encouragement and understanding.

I am also thankful for the friends I made at the Reactor Instituut. Edward, Martina, Zhimin, Harish and Loic with whom I interacted often and spent a lot of time with, have been great friends.

Finally, I would like to thank my family, who have made a lot of sacrifices to see me in this position. I am extremely grateful for their constant support, love and care, without which I could not have completed this Masters study.

I hope to have lent a positive experience to everyone around me and I hope that this project serves well for any person who is interested.

Many Thanks,  
Santhosh Shetty

# List of Figures

1.1	The orientation of different atoms of the G and M residues of the alginate is shown [1].	3
1.2	The characteristic peaks show the formation of side-effects in a Lithium alginate based solid polymer electrolyte cell with Lithium as the anode and Copper as the cathode. . .	4
2.1	The two dimensional radial distribution function of $Na^+$ ion around alginate chain peaks between 0.47 nm and 0.57 nm from alginate chain which is in close agreement with [2].	7
3.1	<b>A.</b> 12 Guluronate residues connected end-to-end. <b>B.</b> Polyguluronate chain with glycosidic bond across periodic boundary to simulate an infinite chain. The long glycosidic bond shown is a misrepresentation due to Avogadro's [3] inability to consider periodic boundary conditions. However, in reality the bonds are much shorter. . . . .	9
3.2	Guluronate residue with oxygen anion on C6 carbon atom. The atoms enclosed in dotted lines are exclusive of the residue and form part of connecting residues. . . . .	10
3.3	X-Ray Diffraction of Lithium Alginate Powder indicating tendency to crystallize. . . . .	11
3.4	16 chains of alginate. <b>A.</b> Top-profile. <b>B.</b> Side-profile. <b>C.</b> Orthogonal Profile. . . . .	13
3.5	Diffusion of $Na^+$ ion in three dimensional space with only $Na^+$ ions neutralizing alginate chains. The slope of the graph is the diffusion constant ( $0.006 \text{ nm}^2 \text{ ns}^{-1}$ ). . . . .	15
3.6	The D-H-A angle should be at least $135^\circ$ and the distance between H-A must be at most 0.25 nm for a two-centered hydrogen bond. . . . .	15
4.1	Guluronate residue with the different oxygen atoms. . . . .	17
4.2	The radial distribution function of Oxygen atoms around $Na^+$ ion peaks at 0.231 nm from $Na^+$ ion for the simulation 3. . . . .	18
4.3	The histogram of Na-O bond lengths peaks at 0.195 nm [4]. . . . .	18
4.4	The interaction energies of $Na^+$ ion with the different oxygen atoms for the simulation 3 indicates $Na^+$ ion interacts preferentially with O2 atom of the residue. . . . .	19
4.5	Distance between O2 and O3 is larger than the typical distance between $Na^+$ ion and oxygen atom. The distance between O61 and O62 is much lower as they are situated on the same carbon C6 atom. . . . .	19
4.6	Hydrogen bond is shown from H2 of one residue to O61 of the next residue [2]. . . . .	20
4.7	The variation of interaction energies of $Na^+$ ion with O2, O3, O61 and O62 atoms for all simulations at 300K. Across all simulations, $Na^+$ ion interacts preferentially with O2 as opposed to O61 or O62. . . . .	21
4.8	The variation of interaction energies of $Ca^{2+}$ ion with O2, O3, O61 and O62 atoms for all simulations at 300K. This indicates that $Ca^{2+}$ ion interacts preferentially with the combination of O61 and O62 atoms compared to O3. . . . .	21
4.10	Variation of distance between 42 <sup>nd</sup> $Na^+$ ion and a set of oxygen atoms over the entire simulation period for simulation 3. . . . .	22
4.9	Nearest Distance from 42 <sup>nd</sup> $Na^+$ ion at every instant along with the nearest atom in simulation 3. The hue of the scatter point indicates a specific oxygen atom, the residue and the chain it is present on and also the type of oxygen atom (O2, O3, O61 or O62). The change in intensity of the scatter plot at around 725 ps indicates a change in the nearest oxygen atoms surrounding the $Na^+$ ion. . . . .	23
4.11	Variation of distance between 42 <sup>nd</sup> $Na^+$ ion and a set of oxygen atoms over period of transition for simulation 3. The 42 <sup>nd</sup> $Na^+$ ion approximately moves from the O62 atom on the third residue of the third chain to the O62 atom on the third residue of the first chain in the time period of around 710 ps to 740 ps. . . . .	24
4.12	Distance between O62 atom on the third residue of the third chain and the O62 atom on the third residue of the first chain remains relatively constant in simulation 3. . . . .	24

---

4.13	Snapshots at progressive time intervals of simulation 3 showing the movement of 42 <sup>nd</sup> $Na^+$ ion from $O62$ atom (yellow) of one residue to $O62$ atom (orange) of another residue. In the inset of each image is the time at which the snapshot was taken. Blue lines in the background indicate the rectangular periodic boundary. The $Na^+$ ion approximately moves from the $O62$ atom on the third residue of the third chain to the $O61$ atom on the third residue of the first chain in the duration of around 710 $ps$ to 740 $ps$ [5]. . . .	25
4.14	At 300 K, the diffusion constant of $Na^+$ ion drops by around 48% as $Ca^{2+}$ ion concentration increases to 14.29%. At 373 K, the diffusion constant of $Na^+$ ion drops by around 18.3% as $Ca^{2+}$ ion concentration increases to 14.29%. . . . .	26
5.1	Guluronate residue with the different oxygen atoms. . . . .	28
A.1	Working Directory Structure for Molecular Dynamics in GROMOS. . . . .	31
A.2	The process of generation of required number of alginate chains. . . . .	38
A.3	<b>sim_box_alginate.cnf</b> . . . . .	41
A.4	<b>sim_box_alginate.por</b> . . . . .	41
A.5	<b>sim_box_alginate.rpr</b> . . . . .	41

# List of Tables

2.1	Diffusion Constant of $Na^+$ ion in z-direction calculated in the re-implemented version is in close agreement with that of [2]. . . . .	6
3.1	Summary of simulated systems along with their compositions at different temperatures.	12
3.2	Increasing temperature steps in equilibration and associated simulation time. . . . .	13
4.1	List of atoms, their mass and charge in guluronate residue and neutralized system. . .	17
4.2	The diffusion coefficients are calculated from a linear least-square fit of mean square displacements over the time-period 0 to 3 ns, each of them calculated over the entire simulation period of 10 ns considering all time-origins. The ionic diffusion can be three-dimensional ( $D_{xyz}$ ) or transverse ( $D_{xy}$ ) or longitudinal ( $D_z$ ) and is averaged over all ions of its type. The error estimate is given by the standard deviation divided by square root of the number of ions as shown in parentheses. [2] . . . . .	26
4.3	Diffusion Constant calculated for PEO (Polyethylene Oxide) system in [6] is compared with the sodium alginate system under analysis at 373 K . . . . .	27



# Contents

<b>List of Figures</b>	<b>iv</b>
<b>List of Tables</b>	<b>vi</b>
<b>List of Abbreviations</b>	<b>1</b>
<b>1 Introduction</b>	<b>2</b>
1.1 Solid Electrolyte Batteries . . . . .	2
1.2 Structure of Alginates . . . . .	2
1.3 Experimental Work . . . . .	3
1.4 Research Objectives . . . . .	4
1.5 Structure of Document . . . . .	4
<b>2 Background Work on MD of Alginates</b>	<b>5</b>
2.1 Existing Computational Analysis Techniques . . . . .	5
2.2 Computational Analysis Techniques for Polymer Electrolytes . . . . .	5
2.3 Molecular Dynamics of Alginates . . . . .	6
2.3.1 Alginate in water . . . . .	6
2.3.2 Diffusion Constant . . . . .	6
2.3.3 Radial Distribution Function . . . . .	7
<b>3 Alginate Polymer Electrolyte Simulations</b>	<b>8</b>
3.1 Description of MD Simulations . . . . .	8
3.1.1 Structural Setup . . . . .	8
3.1.2 Parameters and settings for Simulation . . . . .	11
3.1.3 Simulation Experiments . . . . .	12
3.2 Simulation Procedure . . . . .	12
3.2.1 Topology Generation . . . . .	12
3.2.2 Co-ordinate Generation . . . . .	12
3.2.3 Minimization of the solute . . . . .	12
3.2.4 Solvation of the solute . . . . .	12
3.2.5 Ionization for neutralization . . . . .	13
3.2.6 Equilibration of molecular system . . . . .	13
3.2.7 Molecular Dynamics . . . . .	13
3.3 Tools for Analysis . . . . .	13
3.3.1 Interaction Energy . . . . .	14
3.3.2 Minimum Distance Function . . . . .	14
3.3.3 Diffusion Constant . . . . .	14
3.3.4 Radial Distribution Function . . . . .	14
3.3.5 Hydrogen Bond . . . . .	14
<b>4 Results of MD Simulation</b>	<b>16</b>
4.1 Analysis of the Interaction Energies . . . . .	16
4.1.1 $Na^+$ ion's interaction . . . . .	17
4.1.2 $Na^+$ ion's preferential interaction with <i>O2</i> compared to <i>O61</i> or <i>O62</i> . . . . .	19
4.1.3 $Na^+$ ion's preferential interaction with <i>O2</i> compared to <i>O3</i> . . . . .	20
4.1.4 $Ca^{2+}$ ion's interaction . . . . .	20
4.2 Movement of the Sodium ion . . . . .	22
4.3 Analysis of the Diffusion Constant . . . . .	26

---

<b>5</b>	<b>Conclusions and Recommendations</b>	<b>28</b>
5.1	Conclusions . . . . .	28
5.2	Future Work. . . . .	29
<b>A</b>	<b>Polymer Electrolyte MD Implementation in GROMOS Manual</b>	<b>30</b>
A.1	Step-Wise Implementation . . . . .	30
A.2	Topology Generation . . . . .	33
A.3	Co-ordinate Generation . . . . .	36
A.4	Minimization of the Solute . . . . .	39
A.5	Solvation of the solute . . . . .	40
A.6	Ionization for neutralization . . . . .	42
A.7	Equilibration of molecular system. . . . .	43
A.8	Molecular Dynamics . . . . .	45
	<b>Bibliography</b>	<b>46</b>

# List of Abbreviations

- MD - Molecular Dynamics
- rdf - Radial Distribution Function
- mdf - Minimum Distance Function
- LiB - Lithium-ion Battery
- PEO - Polyethylene Oxide

# 1

## Introduction

*This chapter details the necessity of solid electrolyte batteries in Section 1.1. The structure of alginates has been discussed in Section 1.2. The experimental work that led to transition towards a computational approach is explained in Section 1.3. The research objectives and questions that are attempted to answered through this thesis are mentioned in Section 1.4. The rest of the document's structure is outlined in Section 1.5.*

### 1.1. Solid Electrolyte Batteries

Lithium-ion batteries (LiB) have great advantages such as long cycle-life, high energy density [7] and these have made it a remarkable energy storage device. Today, it is used in many consumer products such as electric vehicles, mobile phones and even stationary energy storage systems.

Despite the numerous advantages these traditional LiBs possess, they face one serious shortcoming: LiBs are susceptible to fire accidents as the organic liquid electrolytes have high flammability [8]. Hence, traditional LiBs are not safe and solid-state batteries can be utilized. The packaging can be reduced leading to increase in energy density. Finally, solid-state batteries have excellent mechanical properties. Apart from this solid-state batteries can make the usage of Li-S batteries possible which are higher in density than LiBs. Li-S batteries with liquid electrolytes suffer from dissolution of cathode material [9]. This leads to loss of active material. A solid electrolyte would prevent any dissolution. Solid electrolytes can also largely prevent dendrite formation in Lithium-ion batteries [10].

Solid electrolytes form an important part of the solid-state battery. They can either be inorganic or organic. Inorganic solid electrolytes are plenty and the prominent ones are NASICON, perovskite, argyrodite, LISICON etc [11], [12], [13]. Organic or polymer electrolytes are further divided into solid polymer electrolytes and gel polymer electrolytes [14]. PEO based electrolytes are prominent examples of polymer electrolytes. Solid polymer electrolytes can reach conductivities of up to  $10^{-5} S cm^{-1}$  while gel polymer electrolytes can reach conductivities of the order of  $10^{-3} S cm^{-1}$  by inserting fillers and application of other modification techniques [14]. Solid polymer electrolytes also have wider electrochemical and thermal stability window [15], [16].

### 1.2. Structure of Alginates

Alginates are naturally occurring polymers in cell walls of seaweed. They are predominantly present to provide flexibility. Alginates are used in food applications, given its low cost, and also in biomedical applications, given its compatible with biological systems.

Alginates are also utilized in Li-ion batteries. The degradation of anode is prevented by mixing alginate with Silicon nanopowder [17]. This allows the diffusion of  $Li^+$  ions while keeping the Silicon nanoparticles bounded to the Copper collector enabling good electronic conductivity. Alginates are also used as binders in graphite electrodes [18]. Alginate based binders are also used to suppress voltage and capacity fading in [19].

Alginates are hetero-polysaccharides formed from (1,4)-linked  $\beta$ -D-mannuronate (M) and  $\alpha$ -L-guluronate (G) residues [20] as shown in Fig. 1.1. These two residues are C5 epimers and differ in the orientation of the  $-OH$  group on the C5 atom. Apart from this, they possess different conformations;

D-mannuronate has  ${}^4C_1$  conformation with  $4^{th}$  carbon atom facing up and the  $1^{st}$  carbon atom facing down. On the contrary, L-mannuronate has  ${}^1C_4$  conformation with  $4^{th}$  carbon atom facing down and the  $1^{st}$  carbon atom facing up.

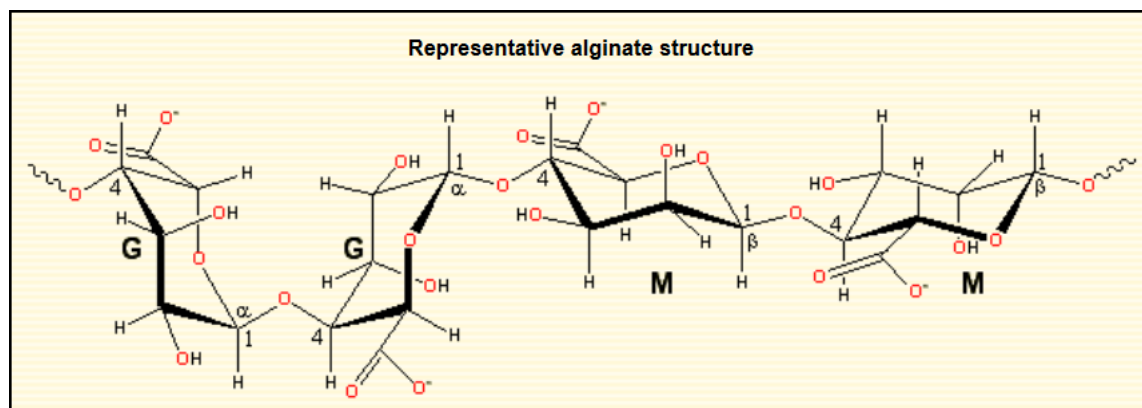


Figure 1.1: The orientation of different atoms of the G and M residues of the alginate is shown [1].

Polyguluronate segments are believed to be responsible for junction zones [21]. Junction zones are those regions where a cross-linking ion interacts with two adjacent G residues of one chain and two other G residues in the opposite chain. Gelation mainly happens in alginates through divalent metal cations and carboxylate groups. The polyguluronate gelation mechanism through Calcium ions is described as an egg-box model [22].

### 1.3. Experimental Work

Lithium Alginate was synthesized by neutralizing 0.1 M Lithium Hydroxide with Alginic Acid. 50% glycerol was added by weight as a plasticizer to allow for mechanical flexibility. This was then laid out in a plastic petridish on a level surface and heated to remove any water. Finally, this gel type film was transferred into a vacuum oven where it was kept overnight to remove all water. After this, the Lithium Alginate film was formed.

Electrochemical Impedance spectroscopy revealed that the film has a conductivity of about  $10^{-6} S cm^{-1}$ . A full cell was made with Lithium Alginate film as the solid polymer electrolyte, Lithium metal as the anode and Copper as the cathode. The cell was able to pass a small discharge current of about 10 nA as shown in Fig. 1.2. However, the cell potential never reached 0 V upon discharge with characteristic peaks appearing as discharge occurred. This led to the conclusion that there is a presence of side-effect formation that is not understandable. To further understand the effects of alginate polymer functioning as an electrolyte, it was decided to carry out MD simulations.

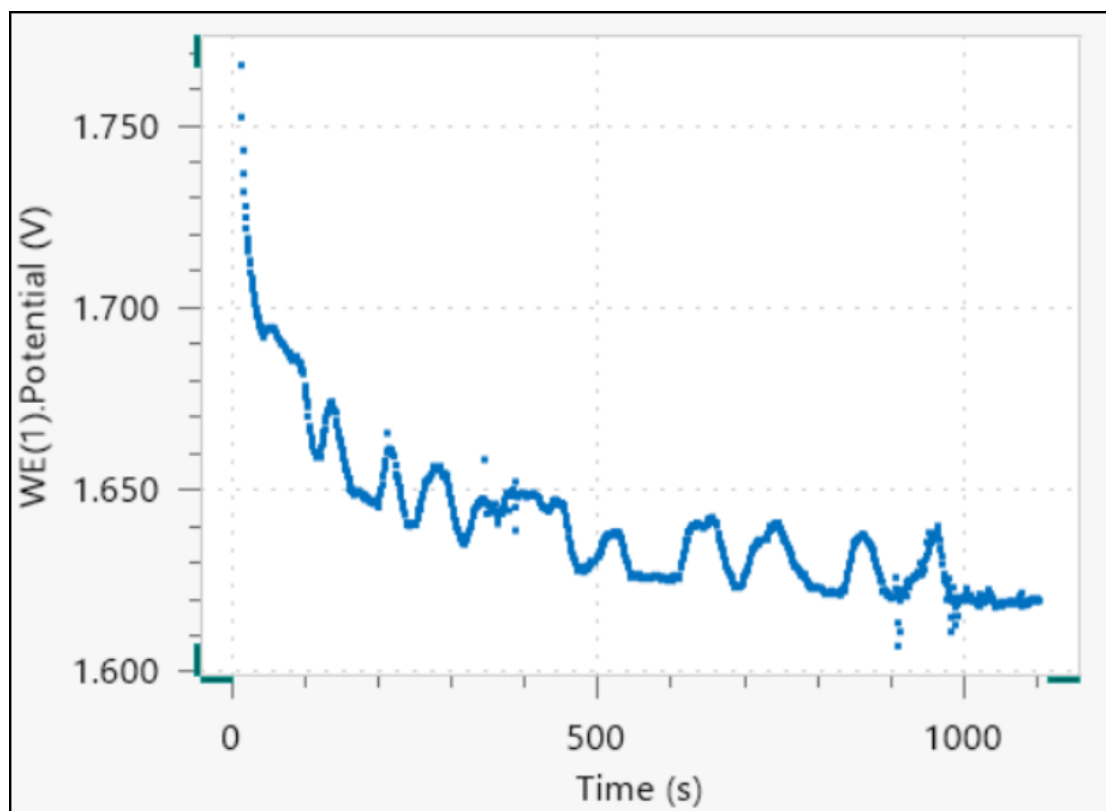


Figure 1.2: The characteristic peaks show the formation of side-effects in a Lithium alginate based solid polymer electrolyte cell with Lithium as the anode and Copper as the cathode.

## 1.4. Research Objectives

The purpose of this thesis is to study the feasibility of alginate as polymer electrolytes through molecular dynamics simulations. For ease of implementation, sodium alginate is utilized as the system under test. The main research question is:

**Can sodium alginate be used as a polymer electrolyte?**

The sub-questions that can be answered are:

1. How does calcium concentration affect the diffusion of the sodium ion?
2. How does the temperature affect the diffusion of the sodium ion?
3. What are the major interactions associated with the sodium ion and how do they affect the movement of the sodium ion?

## 1.5. Structure of Document

The rest of the document is structured in the following manner. Chapter 2 reviews some of the literature present on computational analysis techniques in general and specifically, for alginate molecules. In Chapter 3, the simulations carried out are described in detail. The results of the simulations are presented and discussed in Chapter 4. Chapter 5 presents the conclusions drawn from the simulations. Recommendations are also provided on increasing the accuracy of the simulation techniques and performing experiments for the validation of the same. Appendix A contains a comprehensive manual for establishing any desired simulation of a polymer electrolyte using GROMOS software.

# 2

## Background Work on MD of Alginates

*The main research question was established in Chapter 1. This chapter details the prior work done on using molecular dynamics for polymer electrolytes. In Section 2.1, the popular molecular dynamics techniques used are discussed. The molecular dynamics techniques used for polymer electrolytes are specified in Section 2.2. The molecular dynamics technique that was used for alginates prior to this work is discussed and validated in Section 2.3.*

### 2.1. Existing Computational Analysis Techniques

Molecular dynamics simulations that use software to approximate the movements of particles such as atoms, ions and molecules using equations of motion and force-fields. These particles are allowed to interact with each other over a fixed period of time at desired temperatures. Following this, the energies and the trajectories taken by these particles are studied in detail to gain an understanding of how these systems might work in reality. As there are large number of particles, it is impossible to solve the equations analytically. Computer softwares take the numerical approach to solve these equations subject to boundary conditions. As a result, numerical errors aggregate over time. Hence, careful selection of parameters to ensure the removal of these errors or of any large incomputable forces must be eliminated.

One of the approaches to MD techniques is known as ab initio molecular dynamics. It does not require any description of force-fields. By utilizing the information of the electronic structure of various atoms, the different forces are computed [23]. However, ab initio molecular dynamics is computationally expensive and does not scale to systems such as polymers which contain large number of atoms.

The alternative approach is to utilize force-field description. A standard force-field is designated and all equations of motion are solved using these defined fields. Large-scale simulations of long polymer chains can be computed using relatively lesser computational resources. Atomistic approaches are not exact but provide a good enough compromise between accuracy and computational resources [24]. Hence, for the purposes of ion transport in polymer electrolytes, this project focuses on the usage of force-field based techniques.

### 2.2. Computational Analysis Techniques for Polymer Electrolytes

Monte-Carlo techniques are also popular methods for establishing simulations of polymer electrolytes [25], [6]. MD simulations for polymer electrolytes have focused primarily on PEO-based electrolytes [24]. PEO with Lithium Bromide and Zinc Bromide salt concentrations were simulated at different temperatures in [26]. The structural and dynamical properties of lithium iodide in PEO were studied in [27]. Apart from the movement of the positive ion, it was also found that the anion motion was related to the PEO motion [24]. Cation hopping events were identified within polymer segments [28]. Lithium ion diffusion coefficient contribution from different mechanisms in polymer structures were found [29].

There are many simulation softwares for conducting molecular dynamics on polymers. Prominent ones are CHARMM [30], GROMOS [31], AMBER [32]. Open-source softwares such as GROMACS [33] did not have force-fields for alginate structures and hence was difficult to adapt to. It was decided to use GROMOS as the choice of simulation software for the following reasons:

- Well structured documentation is available at reach. As a result, requisite parameters can be optimized well and tuned easily.
- Existing resource of simulation of alginates in the form of Perić-Hassler & Hünenberger's past work on simulation of alginates in water using GROMOS [2].

GROMOS uses a united-atom force field. This means any hydrogen atom associated with a carbon atom is considered as a single entity and has a separate force-field defined for it.

## 2.3. Molecular Dynamics of Alginates

Perić-Hassler & Hünenberger's past work on simulation of alginates uses a system of single alginate chain surrounded with water. It was necessary to re-implement the work in [2] for the following reasons:

1. To validate the settings of the model specified by cross-verifying the results obtained in the re-implementation with that of the original work. This is helpful in weeding out any possible discrepancies in parameter setting.
2. To gain knowledge of the linkage of the different residues of the alginate chain. This is helpful in the creation of a multi-chain structure.

### 2.3.1. Alginate in water

Alginates were simulated using GROMOS biomolecular simulation software, in a solvent environment of water in [2]. To approximate reality as close as possible, the chain was made infinite by using periodic boundary conditions. This eliminates chain-end effects. Here, a single alginate chain consisting of a repeat unit of 12 guluronate residues connected end-to-end was aligned along the z-axis and a glycosidic bond was made across the periodic boundary. This forms a cyclic topology.

The single-chain alginate is solvated with water and around 12  $Na^+$  ions are inserted to neutralize the system. The parameters and the methodology of simulation were kept identical to [2]. Finally, the results that were obtained in this simulation were compared to the original.

Two main characteristics of the simulation were examined:

1. Diffusion Constant
2. Radial Distribution Function

### 2.3.2. Diffusion Constant

Diffusion constant is calculated by taking a linear least-squares fit of the mean square displacements over a time-period of 0 to 3  $ns$ . The mean square displacements are averaged over 0 to 10  $ns$  by considering all time origins.

Table 2.1: Diffusion Constant of  $Na^+$  ion in z-direction calculated in the re-implemented version is in close agreement with that of [2].

<b>Sodium Alginate in Water</b>	$D_z$ ( $nm^2 ns^{-1}$ )
Original System	1.63 (0.16)
Re-implemented	1.95 (0.51)

From Table 2.1, diffusion constant of the  $Na^+$  ion was calculated in the z direction and is validated according to Table 2.1. The diffusion constant in the re-implemented system is within the error estimate of the original work. Hence, the parameter settings have been implemented as specified in [2].



### 2.3.3. Radial Distribution Function

Radial Distribution is the arrangement of sodium ions around the polyguluronate chain. In the original work, the two dimensional radial distribution function of the  $Na^+$  ion around the alginate chain was calculated by taking the helix axis of the alginate chain as the central structure. However, this was a cumbersome process. A simplification with regard to this was made. The center of mass of the alginate chain is calculated and it's  $(x, y)$  co-ordinates are taken as the center. Correspondingly, only the  $(x, y)$  co-ordinates of the  $Na^+$  ion are taken into consideration.

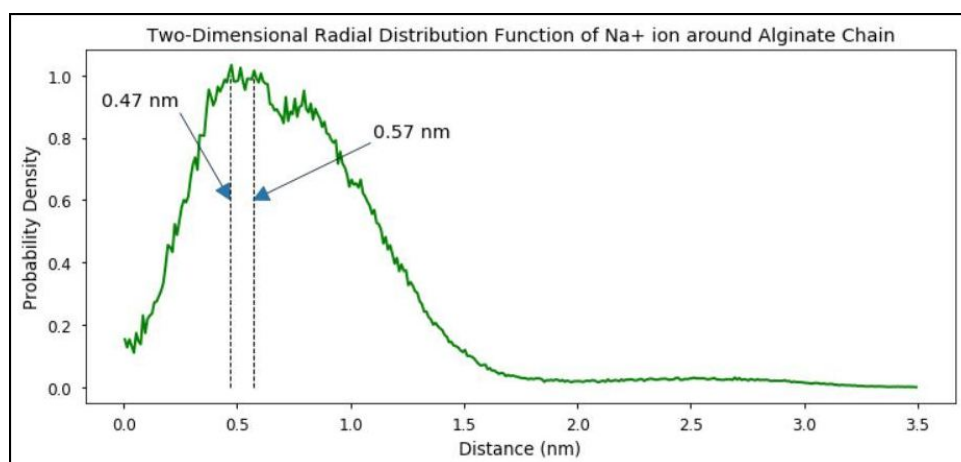


Figure 2.1: The two dimensional radial distribution function of  $Na^+$  ion around alginate chain peaks between 0.47 nm and 0.57 nm from alginate chain which is in close agreement with [2].

From Fig. 2.1, it is seen that the radial distribution function of  $Na^+$  ion around alginate chain peaks at around 0.47 nm to 0.57 nm. This is in close agreement to that seen in the original work in [2]. This discrepancy can be attributed to the simplification of radial distribution function calculation as suggested above.

By conducting this simulation, and from the results obtained in Section 2.3.2 and Section 2.3.3 it was verified that the model parameters used were in close approximation to that of [2]. Using the knowledge gained here, the simulations were adapted to represent polymer electrolytes, specifically, sodium alginate in Chapter 3 using GROMOS software.

# 3

## Alginate Polymer Electrolyte Simulations

*From Chapter 2, it was found that the GROMOS biomolecular simulation software was feasible to conduct molecular dynamics on alginate polymer electrolytes. In this chapter, the methodology of creating various simulations and the analyses that accompany them using GROMOS are specified. Section 3.1 describes the structure of the molecule considered and the specifications associated for each of the simulation. The process of establishing the simulation is detailed in Section 3.2. The methodology of analyzing the outcomes of the simulation are mentioned in Section 3.3.*

*Once the methodology of analyzing the outcomes of the simulation have been outlined accurately, they are discussed in detail in Chapter 4.*

### 3.1. Description of MD Simulations

All MD simulations were carried out using GROMOS96 tool with the GROMOS 45A4 force-field [2].

#### 3.1.1. Structural Setup

A single alginate chain consists of 12 guluronate residues linked end-to-end through oxygen atoms. This chain is of length 5.23 nm. The alginate chain is displayed in Fig. 3.1 A.

For the sake of approximating an infinite chain, the terminal residues are connected through a glycosidic bond through the periodic boundary [34]. This is shown in Fig. 3.1 B.

It was decided to use sodium alginate as the polymer electrolyte as opposed to lithium alginate for the following reasons:

1. Sodium ion non-bonded interaction parameters are defined well in GROMOS force-field whereas the same for Lithium ion are absent.
2. Sodium ion batteries are equally important and can be explored by the use of sodium alginate solid polymer electrolytes.
3. Sodium ion is larger, spherical and well-behaved in terms of force-field based MD capturing its characteristics. However, Lithium ion is very small and may not have feasible characteristics for a force-field based MD.

To approximate possible solid polymer electrolyte conditions, the density of the the system must match with that of reality. For lack of data on density of sodium alginate, it was decided that the alginate chains would be placed in the rectangular periodic boundary box with a density equivalent of that of alginic acid. It was assumed that through the simulation's equilibration phase, the application of atmospheric pressure conditions would bring the system to a density equivalent to that of sodium alginate.

Alginic acid has a density of  $1.6 \text{ g cm}^{-3}$  [35]. This is equivalent to  $1.6 * 10^{-21} \text{ g nm}^{-3}$ . There are two ways to achieve this density:

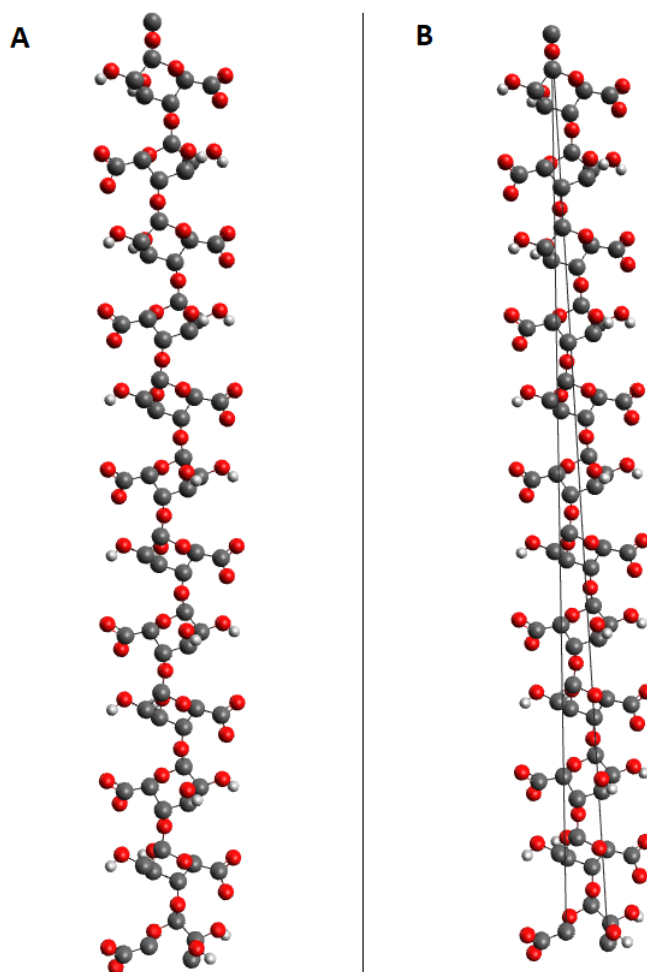


Figure 3.1: **A.** 12 Guluronate residues connected end-to-end. **B.** Polyguluronate chain with glycosidic bond across periodic boundary to simulate an infinite chain. The long glycosidic bond shown is a misrepresentation due to Avogadro's [3] inability to consider periodic boundary conditions. However, in reality the bonds are much shorter.

- Keep a single alginate chain with sodium ions and reduce the box-size to obtain the required density.
- Increase the number of chains such that in a fixed rectangular box size, the required density is reached.

The first option is not viable as the minimum length that can be specified for any dimension must be twice the long-range cutoff distance (a cutoff distance that needs to be specified as an input to the simulation, this was kept to  $1.4 \text{ nm}$ ). Hence, the minimum length of a dimension must be at least greater than  $2.8 \text{ nm}$ . The z-dimension is limited by the length of the chain and is set at  $5.25 \text{ nm}$ . Considering these limitations and the ease of inserting chains, it was decided to increase the number of chains with the box of dimensions  $3.8 \text{ nm} \times 2.9 \text{ nm} \times 5.25 \text{ nm}$ .

The method of addressing this was by inserting enough chains to obtain a density close enough to  $1.6 \times 10^{-21} \text{ g nm}^{-3}$ . For this process, it is necessary to understand the singular component of the polyguluronate chain, the guluronic residue completely. This is shown in Fig . 3.2.

Following are the calculations that decide the number of chains that get inserted into the box:

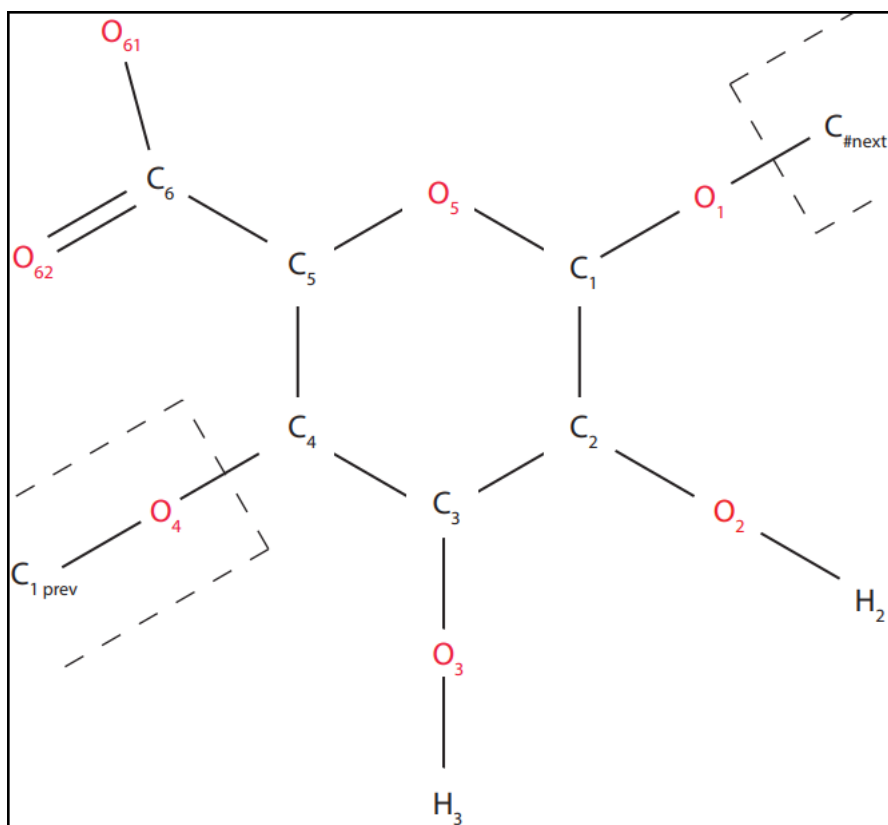


Figure 3.2: Guluronate residue with oxygen anion on C6 carbon atom. The atoms enclosed in dotted lines are exclusive of the residue and form part of connecting residues.

*216.21 g is the mass of 1 mole of residues*

*216.21 g is the mass of  $6.023 \times 10^{23}$  residues*

*$3.59 \times 10^{-22}$  g is the mass of 1 residue*

*Therefore,  $1.6 \times 10^{-21}$  g contains 4.46 residues in  $1 \text{ nm}^3$*

*Hence, in  $3.8 \times 2.9 \times 5.25 = 57.85 \text{ nm}^3$  must contain 257.84 residues*

*Since, each chain contains 12 residues, the system must contain 21.5 chains*

However, for ease of insertion of chains, it was decided that 16 chains will be inserted into the box. The chains are vertically aligned and spaced out from each other at approximately similar distances. X-Ray diffraction of Lithium Alginate, shown in Fig. 3.3, reveals that there are crystallographic peaks in the material which gives rise to the understanding that lithium alginate prefers to align itself in fixed directions. Apart from this, differential scanning calorimetry measurements proved that the glass transition temperature is well beyond  $180^\circ\text{C}$ . These validate the assumption of aligning the polyguluronate chains vertically.

Each of these chains carry 12 negative charges due to the dangling oxygen anions from the carboxylate appendage of the guluronate residue. These must be neutralized. Since, there are 192 negative charges in total, 192 positive charges are inserted to neutralize the system. The exact procedure of establishing the entire structure is laid out in detail in the manual in Appendix A.

The key characteristics of the established structure are:

1. A fixed rectangular periodic boundary box enclosing 16 polyguluronate chains, each consisting of 12 residues.
2. The rectangular box dimensions are  $3.8 \text{ nm} \times 2.9 \text{ nm} \times 5.25 \text{ nm}$ .
3. Each polyguluronate chain is made infinite by connecting terminal residues by a glycosidic bond through the periodic boundary [34].

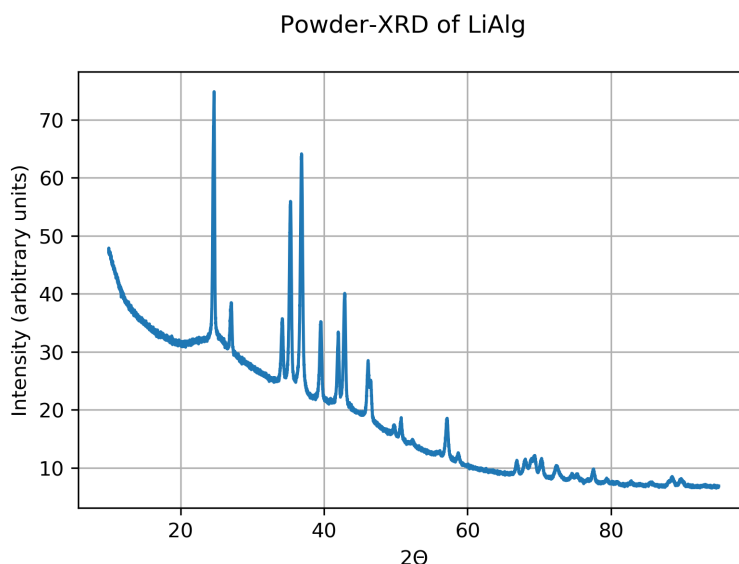


Figure 3.3: X-Ray Diffraction of Lithium Alginate Powder indicating tendency to crystallize.

4. Atmospheric pressure is applied to bring the structure to a density equivalent to that of sodium alginate in reality.
5. The structure comprises of 192 negative charges that need to be neutralized by 192 positive charges.

### 3.1.2. Parameters and settings for Simulation

The following settings were applied for each simulation [References]:

1. The equations of motion use leap-frog scheme based integration with a time step of 2  $fs$  [36].
2. SHAKE algorithm with a relative geometric bond tolerance of  $10^{-4}$  is used for constraining all bond lengths [37].
3. The pressure was maintained at 1 bar by weakly coupling the particle coordinates and the box dimensions to a pressure bath [38]. A relaxation time of 0.5  $ps$ , and isothermal compressibility of  $4.5 \times 10^{-4} kJ^{-1} mol nm^3$  which is suitable for water. This needs to be changed for future work to reflect the value for alginates.
4. The temperature was maintained close to the reference (300 K or 373 K) depending on the simulation, by coupling the degrees of freedom to a heat bath [38] with a relaxation time of 0.1  $ps$ .
5. It is desired to observe all system properties as a virtue of the movement of the atoms and the interactions within themselves rather than due to the movement of the entire system as a whole. Hence, the center of mass motion is removed every 200  $ps$  [2].
6. A twin-range cutoff scheme [39], [40] was specified with short-range and long-range cutoff distances at 0.8  $nm$  and 1.4  $nm$  for non-bonded interaction computation. The short-range pairlist and intermediate-range pairlist were updated every five steps.
7. The reaction-field was corrected to take into account the effect of omitting interactions beyond long-range cut-off distance by using a relative dielectric permittivity of 1 as there is no solvent structure.
8. All simulations were carried out for 10 ns [2].

### 3.1.3. Simulation Experiments

Table 3.1 gives the list of 8 different simulations with variation in the ions involved.

Table 3.1: Summary of simulated systems along with their compositions at different temperatures.

Simulation Code	Number of Sodium ions (Na <sup>+</sup> )	Number of Calcium ions (Ca <sup>2+</sup> )	Percentage of Ca <sup>2+</sup> ions	Temperature (K)
1	192	0	0.0	300
2	192	0	0.0	373
3	168	12	6.67	300
4	168	12	6.67	373
5	144	24	14.29	300
6	144	24	14.29	373
7	120	36	23.08	300
8	120	36	23.08	373

## 3.2. Simulation Procedure

The settings described in Section 3.1.2 are varied as required according to the manual specified in Appendix A. There are six stages to be executed before the final simulation runs:

1. Topology Generation
2. Co-ordinate Generation
3. Minimization of the solute
4. Solvation of the solute
5. Ionization for neutralization
6. Equilibration of molecular system

Simulation 3 is used as an example to illustrate the above stages in detail. The aim of the simulation procedure is to establish a sodium calcium lithium alginate structure at 300K temperature with 6.67% calcium ions.

### 3.2.1. Topology Generation

In this stage, the topology of the polymer molecule is generated. It contains the force-field data concerning the polymer molecule at study. Using individual topology building blocks that are representations of the residue and the ions involved, and the interaction function parameter which contains interactions between all types of atoms, the topology is built. This process is described in Appendix A.

### 3.2.2. Co-ordinate Generation

Once all the topology files are generated, the physical location of each atom needs to be specified. For a single alginate chain, the physical location present in [1] is utilized as specified in the manual in Appendix A. This results in Fig. 3.1. For multiple chains, the custom script developed according to Appendix A is used. This results in Fig. 3.4.

### 3.2.3. Minimization of the solute

Minimization is done to keep the net inter-atomic force on any atom close to zero. This relaxation of energy is necessary to ensure there are no extremely large forces acting in the simulation stage of molecular dynamics. This stage is carried out according to the manual in Appendix A.

### 3.2.4. Solvation of the solute

In real world conditions, any electrolyte in Sodium-ion or Lithium-ion batteries is anhydrous. However, to insert any sodium ions for the simulation 3, water molecules need to be inserted at first. The number of solvent molecules retained is equal to the number of ions that will be inserted later. In this case,

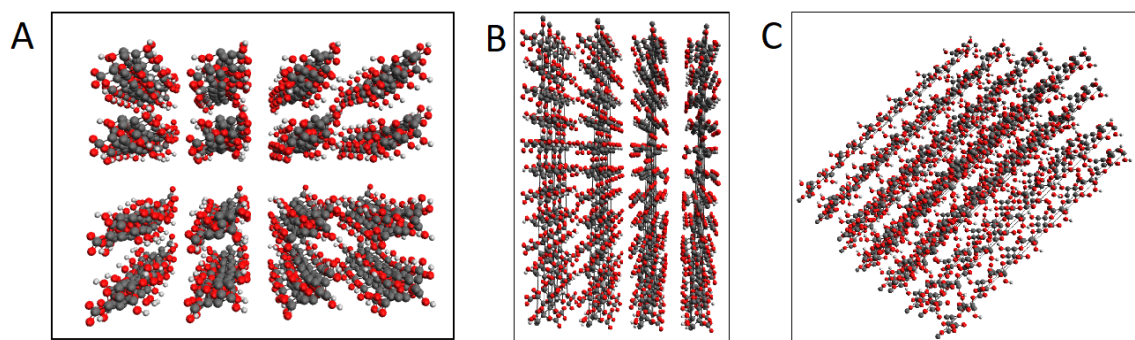


Figure 3.4: 16 chains of alginate. **A.** Top-profile. **B.** Side-profile. **C.** Orthogonal Profile.

the number of solvent molecules to be inserted is 180. The solute-solvent structure is then minimized. Later, the water molecules are substituted by sodium ions or calcium ions as required. This process is described in Appendix A.

### 3.2.5. Ionization for neutralization

In this stage, the solvent molecules that were retained in the previous stage are substituted as required. For the simulation 3, 168  $Na^+$  ions and 12  $Ca^{2+}$  ions are inserted as described in Appendix A.

### 3.2.6. Equilibration of molecular system

In this stage, the system is slowly heated to the simulation temperature. The atoms of the solute are positionally restrained and are slowly loosened up in steps of increasing temperature as specified in Appendix A. If molecular dynamics simulation ran directly at, say, 300K, the atoms of the molecule may be subjected to extremely large forces that GROMOS will not be able to solve and the simulation may crash. For the simulations given in Table 3.1, the simulation proceeds in increasing temperature steps as shown in Table 3.2.

Table 3.2: Increasing temperature steps in equilibration and associated simulation time.

Temperature (K)	Time (ns)
50	0.2
100	0.2
150	0.2
200	0.2
250	0.2
300	0.8
373	0.8

For simulations 1, 3, 5 and 7, only the first six steps in Table 3.2 are executed. For simulations 2, 4, 6 and 8, the seventh step in Table 3.2 is also executed.

### 3.2.7. Molecular Dynamics

Finally, the system is brought to the required simulation temperature of 300K or 373K, the molecular dynamics simulation runs for 10 *ns*. Using the tools described in the following section, various analyses are performed as described in Chapter 4.

## 3.3. Tools for Analysis

The co-ordinates and energies that were printed out during the simulation can be analyzed in various ways. Following are the analyses (tools are specified in [41]) that can be performed within the scope of the research:

1. Interaction Energy

2. Minimum Distance Function
3. Diffusion Constant
4. Radial Distribution Function
5. Hydrogen Bond

### 3.3.1. Interaction Energy

The interaction energy (int-ener) is the nonbonded interaction energy between two sets of atoms. It is a combination of the van der Waal's and electrostatic interactions. In the scope of this thesis, it is of interest to calculate the total interaction energy between ions and the atoms they interact with. This is done using the commands specified in Appendix A. A time-series can also be specified to observe the changes in interaction energy corresponding to two sets of atoms over the time of the simulation. GROMOS calculates the sum total of interaction energy over all ions. However, to calculate the average interaction energy of a particular ion, it needs to be normalized by dividing the total number of ions present.

### 3.3.2. Minimum Distance Function

The minimum distance function (mdf) is a GROMOS tool which lists and calculates, for a given set of atoms, the nearest distance to a second set of atoms. For every atom in the given set, an output time-series of the distance to the nearest atom in the second set along with the atom-specification is printed. In the scope of the thesis, it is of interest to calculate the distance of the sodium ion from the different atoms it interacts with over the simulation timeframe. The method of implementing this on GROMOS is specified in the Appendix A.

### 3.3.3. Diffusion Constant

The diffusion constant (diff) is a measure of the ease of movement of an ion through the system. Here, it also means the rate of spread of the ion. It is measured in the units of  $nm^2 ns^{-1}$  or  $cm^2 s^{-1}$ .

The diffusion coefficients calculation is done by performing a linear fit on the mean square displacements over the time period of 0 to 3 ns. The linear fit rightly rejects the initial build-up of the mean square displacements. This is valid because in the starting of the simulation, the atoms still haven't felt each other and hence they are moving in random straight lines as opposed to movement due to influence from each other. The mean square displacements are calculated on the total simulation time of 10 ns [2] by examining all time origins. As an example, the diffusion of sodium ion in three-dimensional space is shown in Fig. 3.5 for the simulation system 1. Here, the diffusion constant is the slope given by the plot as  $0.006 nm^2 ns^{-1}$ . The plot is also accompanied by an  $R^2$  value, which is a statistical measure of how good the data fits to the regression line.

### 3.3.4. Radial Distribution Function

The radial distribution function (rdf) is a measure of probability of finding an ion at a distance  $r$  away from the reference particle or center of mass point of a set of reference particles.

For measuring the rdf of any ion around a chain, it is desirable to have the reference point as the helical axis of the chain as given in Section 2.3. However, GROMOS by default calculates the rdf differently. Firstly, it assumes the reference point as the center of mass of a set of atoms specified. Using this reference point, a three dimensional rdf is evaluated instead of a two dimensional radial distribution from the helical axis.

To convert the default GROMOS three dimensional rdf into a two dimensional rdf, a simple modification was done. The center of mass point was calculated as earlier. However, only x and y coordinates are used for the calculation of the distribution function as the chain is assumed to be aligned in the z-direction. From Section 2.3, it was shown that this approximation doesn't deviate much from the original calculations.

### 3.3.5. Hydrogen Bond

In GROMOS, a hydrogen bond (hbond) is present if the distance between the hydrogen atom, connected to a donor atom D, is within a distance of 0.25 nm (default setting can be changed) from an acceptor



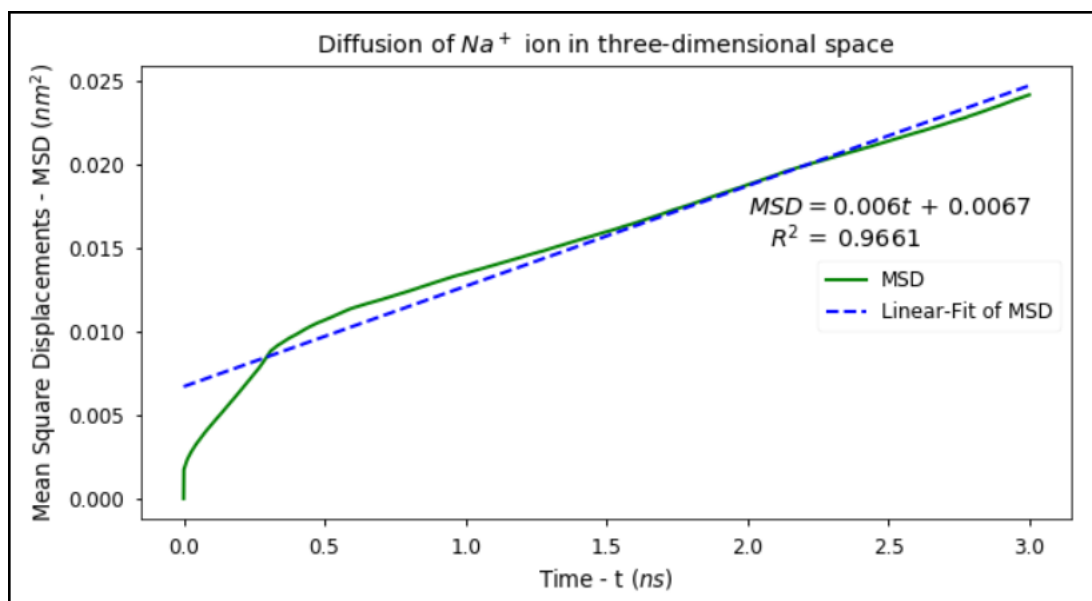


Figure 3.5: Diffusion of Na<sup>+</sup> ion in three dimensional space with only Na<sup>+</sup> ions neutralizing alginate chains. The slope of the graph is the diffusion constant ( $0.006 \text{ nm}^2 \text{ ns}^{-1}$ ).

atom A and the D-H-A angle is larger than  $135^\circ$  (default setting can be changed). This is defined as a two-centered hydrogen bond and is depicted in Fig. 3.6. For this thesis only two-centered hydrogen bonds are considered. The output of this tool is a list of all hydrogen bonds that occur throughout the simulation period and the number of times each of them occur. Information regarding the atoms involved in each of the hydrogen bonds is also specified.

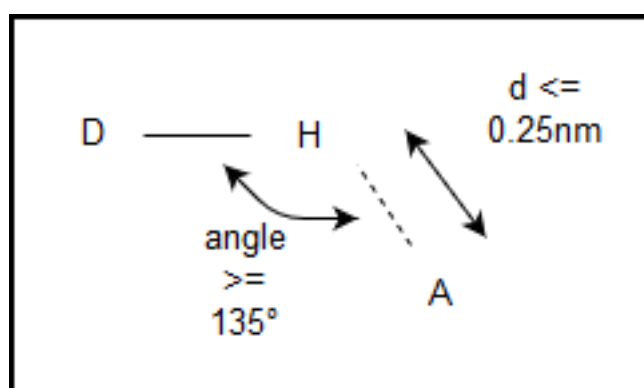


Figure 3.6: The D-H-A angle should be at least  $135^\circ$  and the distance between H-A must be at most  $0.25 \text{ nm}$  for a two-centered hydrogen bond.

# 4

## Results of MD Simulation

*In Chapter 3, the methodology of analyzing the outcomes was specified. Here, each of the outcomes are analyzed accordingly from Section 4.1 to Section 4.3. The results of all the simulations are compared with each other and with previous work where relevant.*

*Using these results, conclusions are drawn and recommendations are provided for future work in Chapter 5.*

Eight simulations with different concentrations of  $Ca^{2+}$  and at two different temperatures of 300 K and 373 K as specified in Table 3.1 were run. Using the tools that GROMOS provides and as mentioned in Section 3.3, the results of the MD simulations can be discussed. The prominent ones are:

1. Analysis of the Interaction Energies
2. Movement of the Sodium Ion
3. Analysis of the Diffusion Constant

### 4.1. Analysis of the Interaction Energies

In this section, the interaction of the two types of inserted positive ions,  $Na^+$  and  $Ca^{2+}$  with the primary negative charge centers are analyzed mainly by using the *int-ener* tool. Other tools such as *rdf* and *hbond* are also utilized to construct arguments for supporting the outputs of interaction energies. The simulation 3 is used as an example to demonstrate the analysis of interaction energies and finally, a comparison is made with the other simulations at the end. All analyses are carried on simulations that run at 300 K.

Oxygen atoms are the primary negative charge centers in the system. The different atoms or ions and their charges present in the guluronate residue in the GROMOS system is given in Table 4.1. The atoms of the guluronate residue are also shown in Fig. 4.1. Some key observations that can be made from this table are:

1. The structure of the guluronate in Fig. 4.1 shows the hexapyranose (6 carbons with a 5-carbon ring). *O1* and *O4* are equivalent and mainly serve as oxygen atoms that link adjacent residues. *O1* and *O5* oxygen atoms are relatively closer to the guluronate backbone than *O2*, *O3* and *O5* oxygen atoms. *O5* is the oxygen atom that completes that 5-carbon ring structure.
2. In Fig. 4.1, the guluronate residue shows *O61* having a single covalent bond and *O62* having two covalent bonds with *C6*. However, from Table 4.1, both *O61* and *O62* carry similar charge leading to the understanding that resonance or stabilisation of the two oxygen atom is assumed.
3. *O1* and *O5* are involved more than one covalent bond with carbon atoms and have lower negative charges than that of *O2*, *O3*, *O61* or *O62* oxygen atoms. This is explained by the fact that in covalent bonds with carbon atoms, the electrons are shared more evenly compared to that of covalent bonds with hydrogen atoms.

Using the *rdf* tool as specified in Section 3.3.4, the three-dimensional radial distribution function for oxygen atoms around the  $Na^+$  ion was found. In Fig. 4.2, we see that the radial distribution function peaks at 0.231 nm from  $Na^+$  ion.

Table 4.1: List of atoms, their mass and charge in guluronate residue and neutralized system.

Atom/ Ion	Mass (amu)	Charge
C3	13.019	0.232
O3	15.994	-0.642
H3	1.08	0.41
C2	13.019	0.232
O2	15.994	-0.642
H2	1.008	0.41
C6	12.011	0.36
O61	15.994	-0.68
O62	15.994	-0.68
C5	13.019	0.376
O5	15.994	-0.48
C1	13.019	0.376
O1	13.019	-0.36
C4	13.019	0.232
NA	22.9898	1.00
CA	40.08	2.00

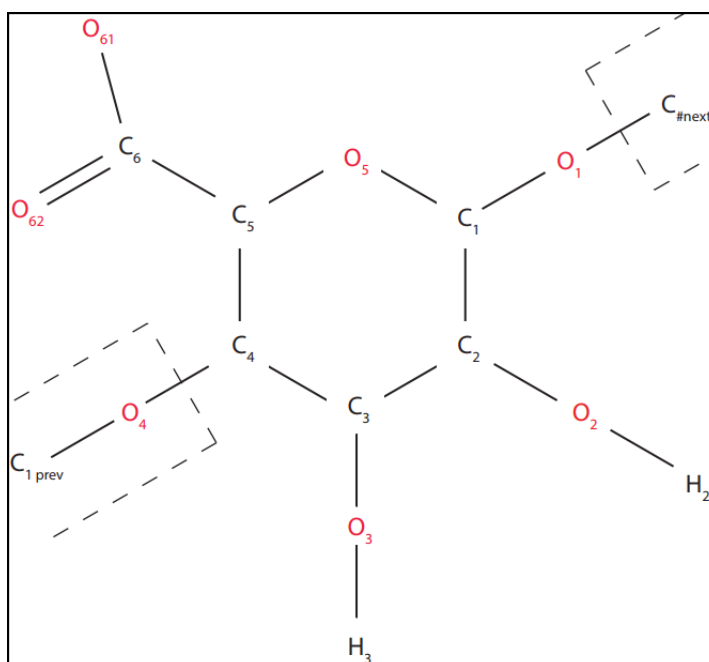


Figure 4.1: Guluronate residue with the different oxygen atoms.

#### 4.1.1.1. $Na^+$ ion's interaction

According to [4], the bond distribution for Na-O bonds peak at 0.195 nm as shown in Fig. 4.3. The reason for considering Na-O bond as opposed to  $Na^+$  ion binding with  $O^{2-}$  ion is because in the guluronate residue as shown in Fig. 4.1, the oxygen atom always has one of its bonds associated either with a hydrogen atom or a carbon atom of the ring. This implies that the sodium ion in the simulated system is in an unbounded state expected to have high enough energy to break free from

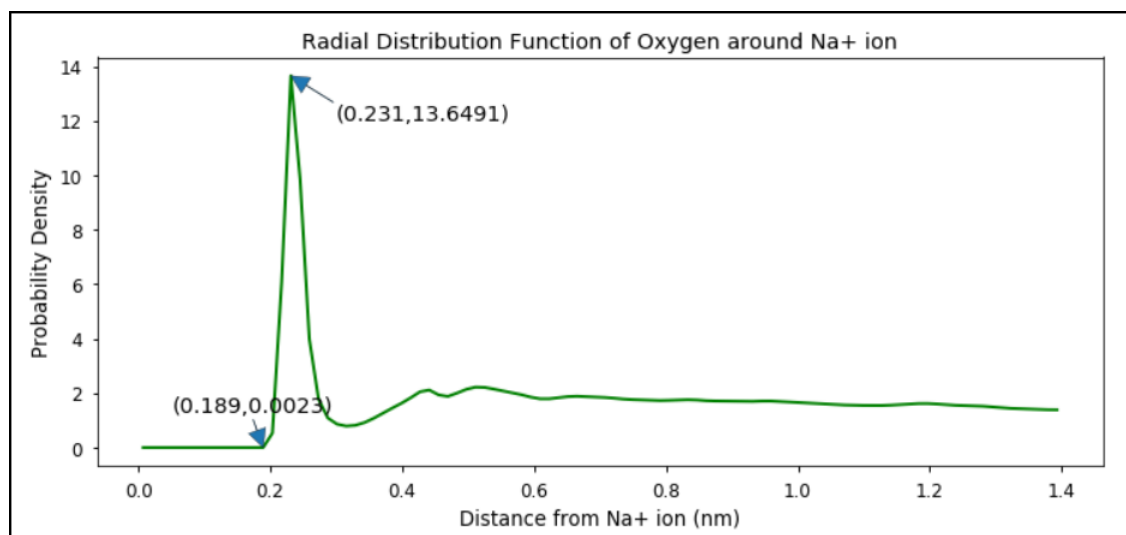


Figure 4.2: The radial distribution function of Oxygen atoms around Na<sup>+</sup> ion peaks at 0.231 nm from Na<sup>+</sup> ion for the simulation 3.

any bond. This is favorable for sodium alginate to function as a polymer electrolyte. Upon executing Section 3.3.1's *int-ener* tool of GROMOS on the output files, the average interaction energy of Na<sup>+</sup> ion with the various oxygen atoms is shown in Fig. 4.4. It was decided to limit the calculation of Na<sup>+</sup> ion - oxygen atom interaction energy to those oxygen atoms which lie within 0.3 nm of Na<sup>+</sup> ion, which is a safe upper limit considering the Na-O bond distribution from Fig. 4.3. This was done to ensure the oxygen atoms present beyond the first sphere of influence (refers to the sphere of radius of length of maximum Na-O bond length) did not play a role. For reference, the different oxygen atoms are shown again in Fig. 4.1. Four prominent points can be concluded from Fig. 4.4:

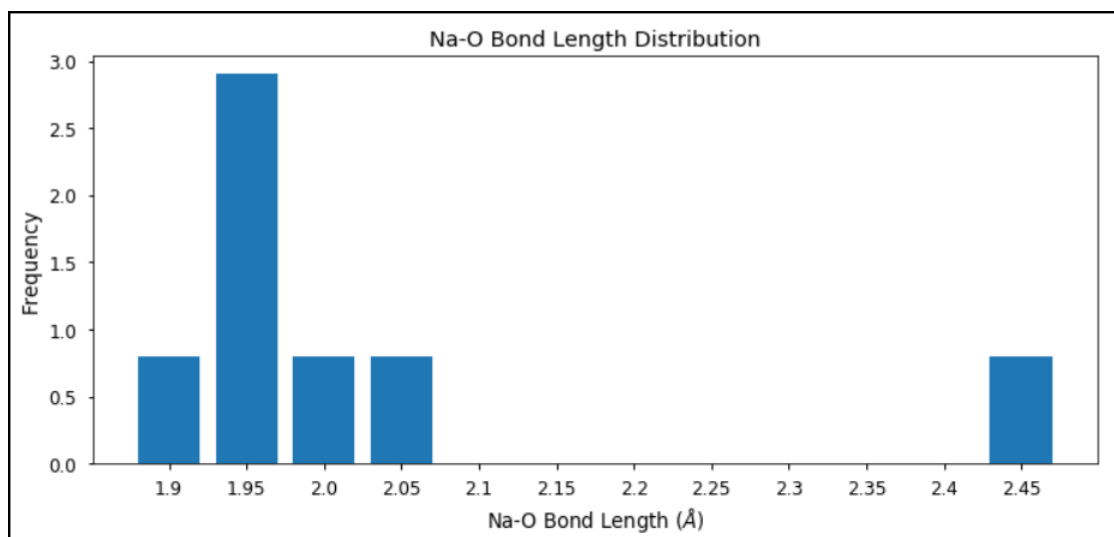


Figure 4.3: The histogram of Na-O bond lengths peaks at 0.195 nm [4].

1. The interaction energies are far higher than the bond dissociation energy of sodium - oxygen which is  $-381 \text{ kJ mol}^{-1}$  [42]. This cross-verifies the statement made earlier in Section 4.1.1 that the sodium ion has enough energy to move as an unbounded particle.
2. O1 and O5 have minimal interaction with Na<sup>+</sup> ion as these oxygen atoms share electrons relatively equally with covalently bonded carbon atoms. This is expected given that they have lesser

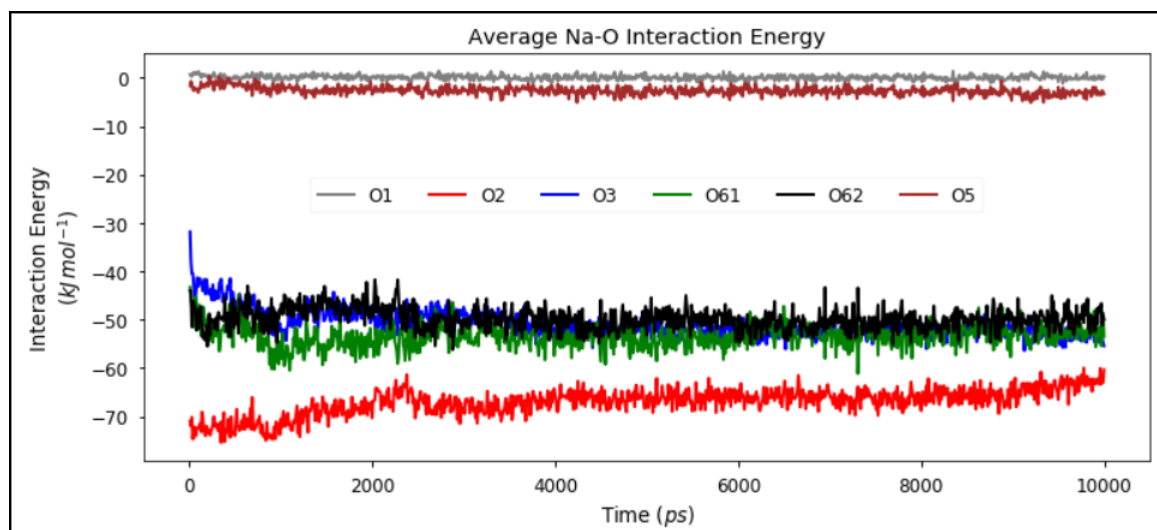


Figure 4.4: The interaction energies of  $Na^+$  ion with the different oxygen atoms for the simulation 3 indicates  $Na^+$  ion interacts preferentially with  $O2$  atom of the residue.

negative charge than the other oxygen atoms as shown in Table 4.1. They primarily serve as linkages for adjacent guluronate residues and as hexapyranose ring oxygen respectively.

- $Na^+$  ion preferentially interacts with  $O2$ , despite  $O61$  and  $O62$  having higher negative charges ( $-0.68$ ) as mentioned in Table 4.1. This is addressed in Section 4.1.2.
- $Na^+$  ion preferentially interacts with  $O2$ , despite  $O2$  and  $O3$  carrying the same charge as shown in Table 4.1. This is addressed in Section 4.1.3.

#### 4.1.2. $Na^+$ ion's preferential interaction with $O2$ compared to $O61$ or $O62$

Since the distance between  $O61$  and  $O62$  atom of the same residue is smaller than the distance between a typical  $Na^+$  ion and oxygen atom as shown in Fig. 4.5, it is likely that the influence of the interaction is spread over  $O61$  and  $O62$  oxygen species. However, the distance between  $O2$  and  $O3$  is larger than the distance between a typical  $Na^+$  ion and oxygen atom. This appears to result in isolated interactions between  $Na^+$  ion &  $O2$  atom, and  $Na^+$  ion &  $O3$  atom respectively. The discrepancy between the interaction of  $Na^+$  ion with  $O2$  and with that of  $O3$  is explained in the following section.

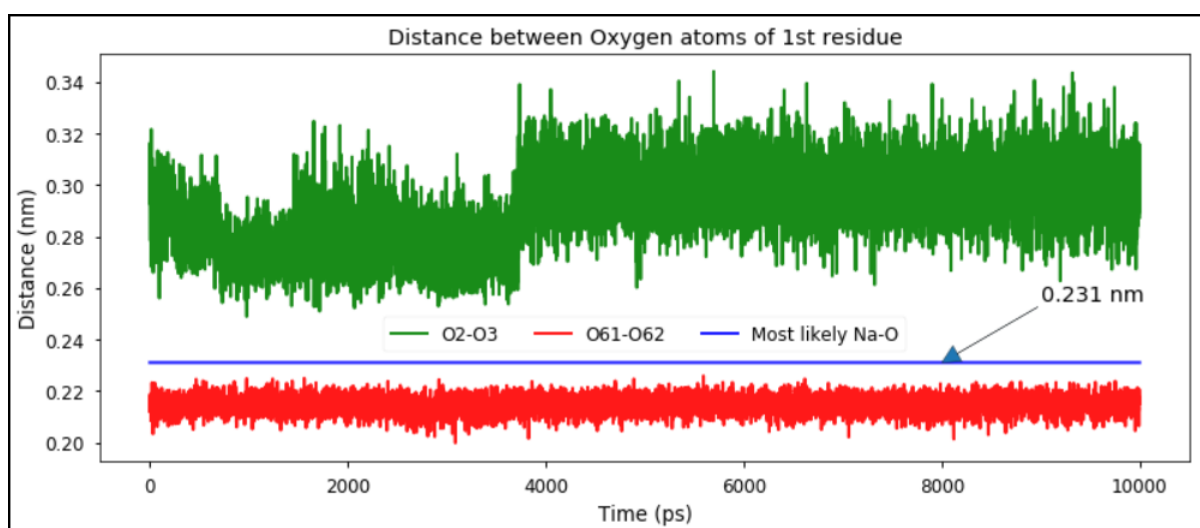


Figure 4.5: Distance between  $O2$  and  $O3$  is larger than the typical distance between  $Na^+$  ion and oxygen atom. The distance between  $O61$  and  $O62$  is much lower as they are situated on the same carbon  $C6$  atom.

### 4.1.3. $Na^+$ ion's preferential interaction with $O2$ compared to $O3$

From Table 4.1,  $O2$  and  $O3$  oxygen atoms have identical charges ( $-0.642$ ), one would expect that they interact identically with  $Na^+$  ion. However, from Fig. 4.4  $Na^+$  ion interacts preferentially with  $O2$  compared to  $O3$  oxygen atom.

Using the *hbond* tool specified in Section 4.1.3, the hydrogen bonds associated with the  $H2$  and  $H3$  atoms of the guluronate residue are found over the entire simulation period. The total number of hydrogen bonds associated with  $H2$  was 0.2 times more than the hydrogen bonds associated with  $H3$ . Hence, it appears that the  $H2$  atom is not as involved with bond formation with  $O2$  compared to  $H3$  atom's involvement with  $O3$ . This appears to lead to a reduction of positive charge around  $O2$  atom which is satisfied by the  $Na^+$  ion. This is a possible explanation of the preferential interaction of  $Na^+$  ion with  $O2$  atom despite  $O3$  having the same charge as that of  $O2$ .

The immediate question that arises as to why do hydrogen bonds form more often at  $H2$  than at  $H3$ . To answer this, the polyguluronate structure is shown in Fig. 4.6. The guluronate residues are in such a manner that the  $H2$  of one residue is closer to the  $O61$  of the next residue. This does not seem to be the case with  $H3$  atom.

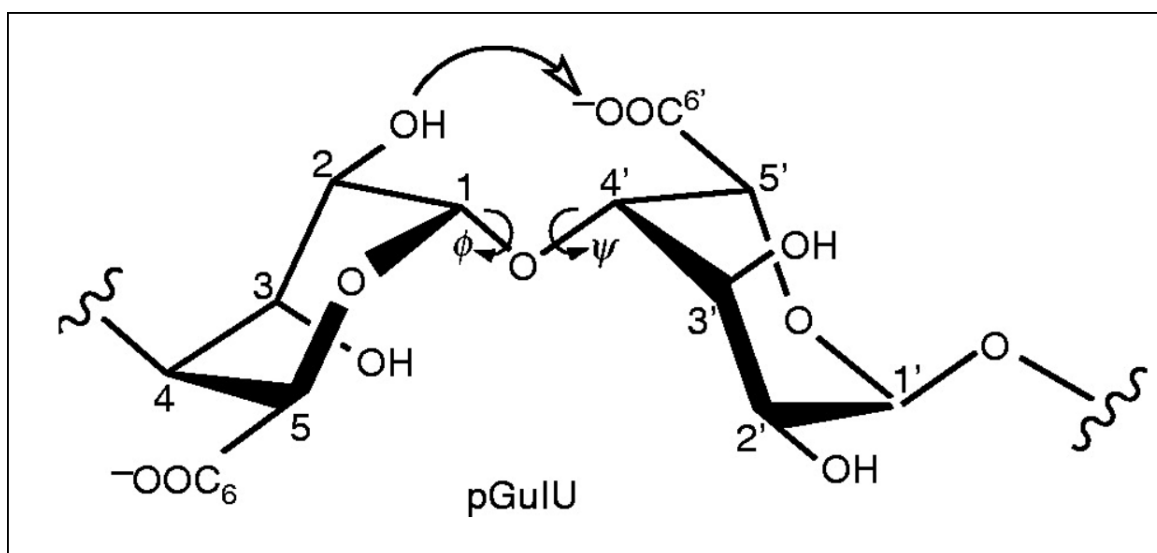


Figure 4.6: Hydrogen bond is shown from  $H2$  of one residue to  $O61$  of the next residue [2].

When checked across the entire set of simulations with varying  $Ca^{2+}$  ion concentrations at 300K, the trend of preferential interaction of  $Na^+$  ion with  $O2$  atom holds as shown in Fig. 4.7.

### 4.1.4. $Ca^{2+}$ ion's interaction

However, the relationships of interaction energies changes when  $Ca^{2+}$  ion is involved.  $Ca^{2+}$  ion preferentially interacts with  $O61$  and  $O62$  compared to  $O2$  and  $O3$ . It appears that this is a possibility because  $Ca^{2+}$  ions need 2 electrons to fall to a lower energy state and this can be provided from a combination of  $O61 - O62$  atoms rather than a single oxygen atom.

The interaction of  $Ca^{2+}$  ion with  $O2$  is comparatively higher than that of  $O2$ . The same explanation provided for  $Na^+$  ion's interaction with  $O2$  in Section 4.1.3 stands. More hydrogen bonds are formed from the  $H2$  atom than  $H3$  atom. Hence,  $Ca^{2+}$  ion appears to neutralize the pronounced electronegativity on  $O2$  rather than  $O3$  atom leading to an increased interaction.

Hence, if  $Ca^{2+}$  ion prefer  $O61$  and  $O62$  atoms and if  $Na^+$  ion prefer  $O2$ , it can be said that  $Ca^{2+}$  ions don't occupy those spots which are responsible for  $Na^+$  ion diffusion.

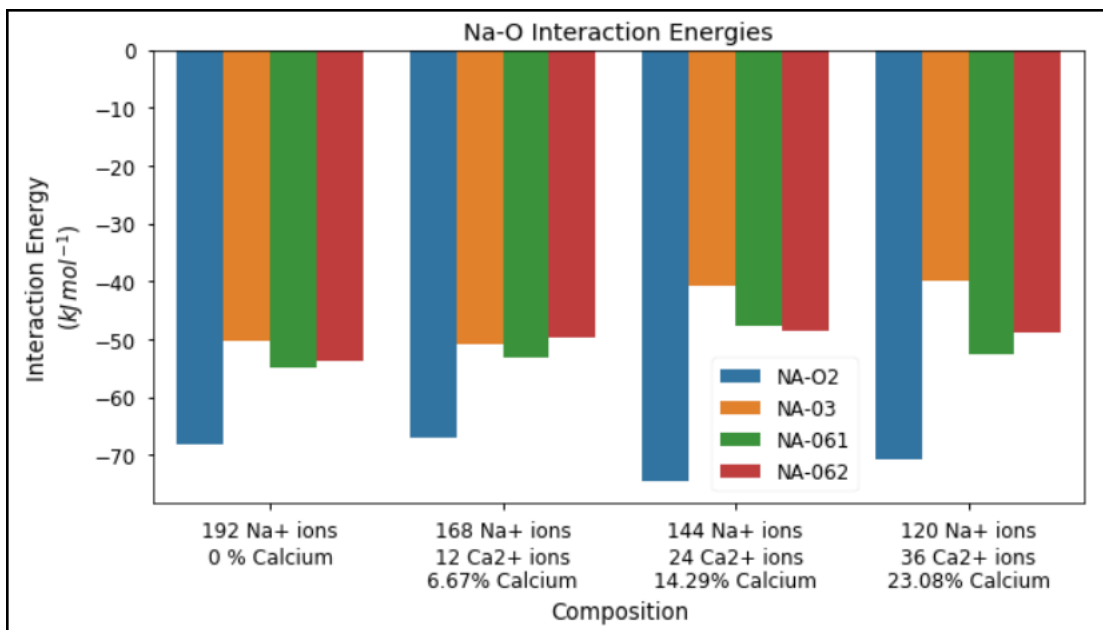


Figure 4.7: The variation of interaction energies of  $Na^+$  ion with  $O_2$ ,  $O_3$ ,  $O_{61}$  and  $O_{62}$  atoms for all simulations at 300K. Across all simulations,  $Na^+$  ion interacts preferentially with  $O_2$  as opposed to  $O_{61}$  or  $O_{62}$ .

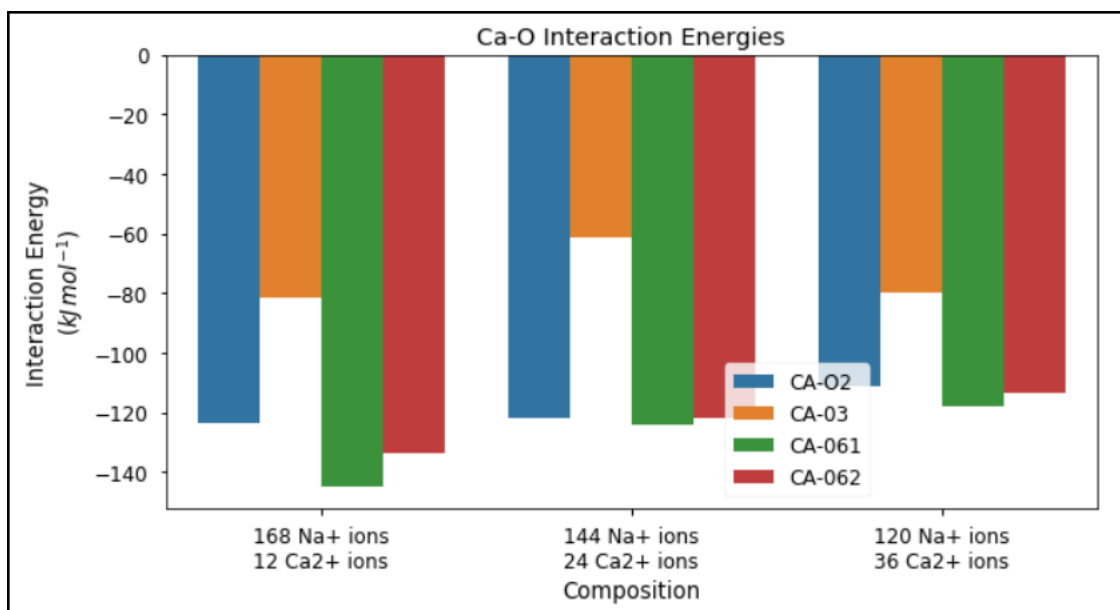


Figure 4.8: The variation of interaction energies of  $Ca^{2+}$  ion with  $O_2$ ,  $O_3$ ,  $O_{61}$  and  $O_{62}$  atoms for all simulations at 300K. This indicates that  $Ca^{2+}$  ion interacts preferentially with the combination of  $O_{61}$  and  $O_{62}$  atoms compared to  $O_3$ .

## 4.2. Movement of the Sodium ion

From Section 4.1, it was clear that the oxygen atoms contributing towards the interaction are  $O2$ ,  $O3$ ,  $O61$  and  $O62$ . Using the mdf tool specified in Section 3.3.2, the nearest distance between an arbitrary  $Na^+$  ion and an oxygen atom from the set of oxygen atoms of  $[O2, O3, O61, O62]$  is found. The specific oxygen which had the nearest distance to  $Na^+$  ion is also found. This is done over the entire simulation period and shown as an example for the 42<sup>nd</sup>  $Na^+$  ion in Fig. 4.9. A transition can be seen at 725 ps in terms of the oxygen atoms surrounding the  $Na^+$  ion by the change in contrast of the scatter points.

To explore in detail the oxygen atoms that are involved the most in the movement of 42<sup>nd</sup>  $Na^+$  ion, distance of the  $Na^+$  ion from a selected list of oxygen atoms is plotted as shown in Fig. 4.10. Since this plot is unclear to show the transition, a smaller window from 700 ps to 770 ps is shown in Fig. 4.11. The movement of  $Na^+$  ion from the  $O62$  atom of the third residue of the third alginic chain to the  $O62$  atom of the third residue of the first alginic chain can be seen.

However, it could also be that the chains themselves move and the  $Na^+$  ion remains stationary. To verify whether this is true, we plot the distance between the  $O62$  atom of the third residue of the third alginic chain and the  $O62$  atom of the third residue of the first alginic chain in Fig. 4.12 between the time period of 710 ps and 740 ps. The change in distance is about 0.15 nm which is much lesser than the distance moved by  $Na^+$  ion which is about 0.8 nm.

However, it must also be mentioned that while these are the oxygen atoms that are most involved in the transition, the movement of  $Na^+$  ion is due to an influence of a combination of oxygen atoms but the contribution from oxygen atoms other than specified is found to be negligible in this particular incidence. A snapshot array of the simulation highlighting the residues and the 42<sup>nd</sup>  $Na^+$  ion involved in movement is shown in Fig. 4.13.

Apart from analyzing the movement of a single  $Na^+$  ion, a diffusion constant analysis can be performed to understand the movement of all  $Na^+$  ions. This is the subject of the following section.

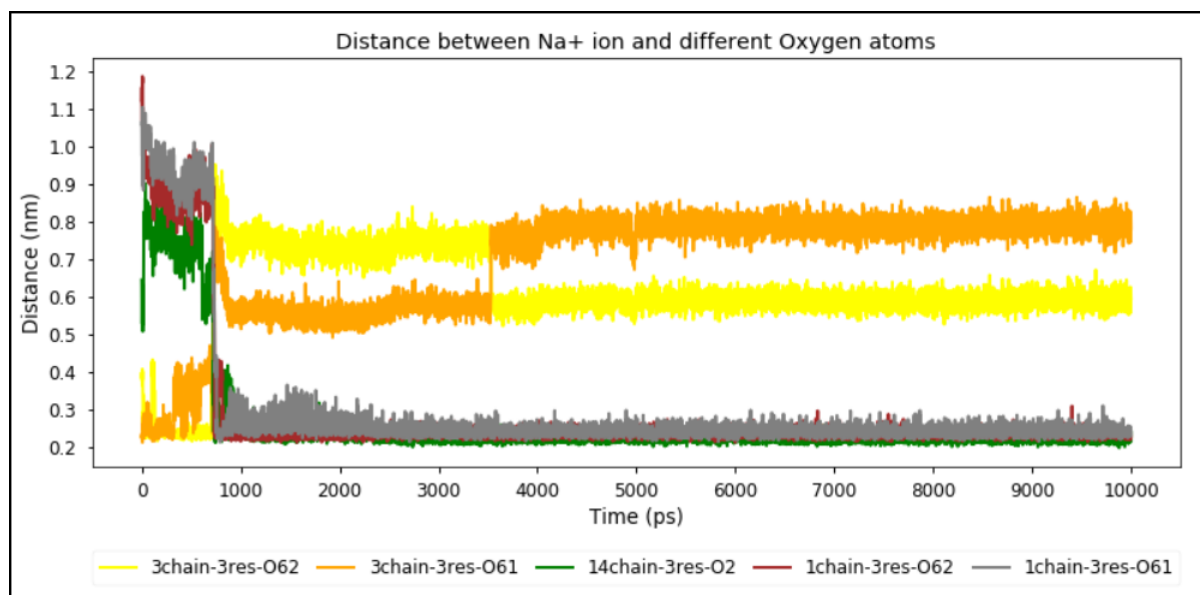


Figure 4.10: Variation of distance between 42<sup>nd</sup>  $Na^+$  ion and a set of oxygen atoms over the entire simulation period for simulation 3.



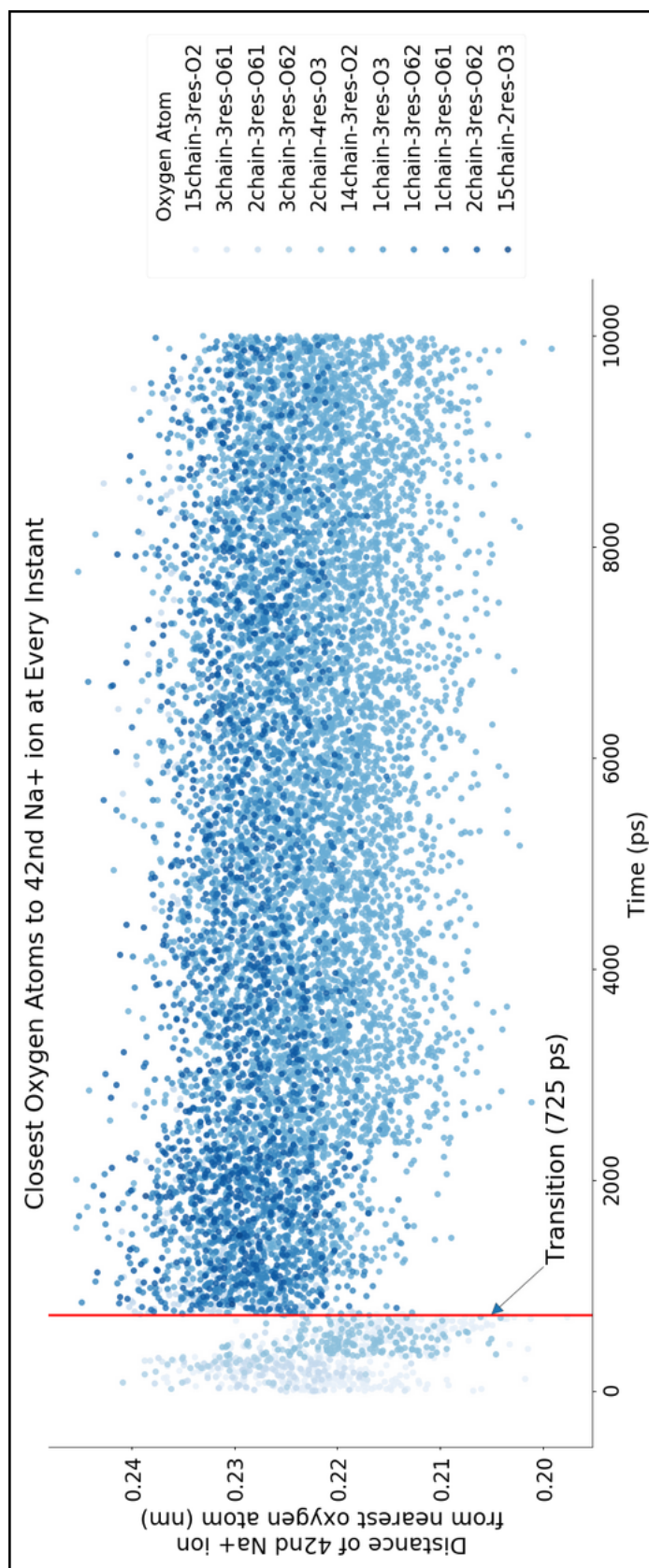


Figure 4.9: Nearest Distance from 42<sup>nd</sup> Na<sup>+</sup> ion at every instant along with the nearest atom in simulation 3. The hue of the scatter point indicates a specific oxygen atom, the residue and the chain it is present on and also the type of oxygen atom (O2, O3, O61 or O62). The change in intensity of the scatter plot at around 725 ps indicates a change in the nearest oxygen atoms surrounding the Na<sup>+</sup> ion.

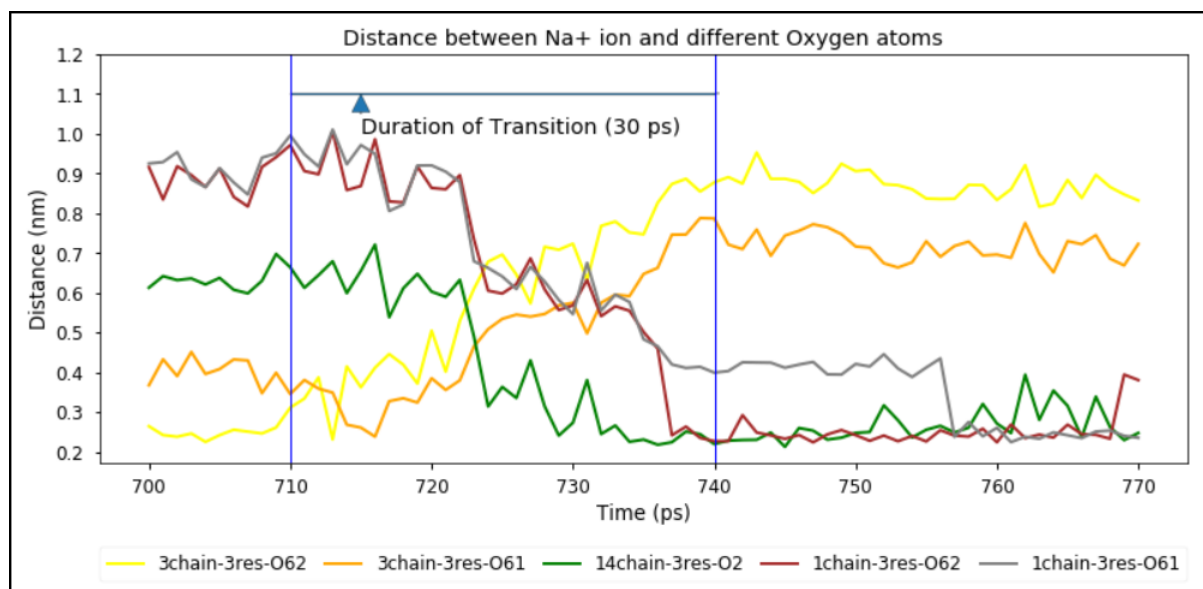


Figure 4.11: Variation of distance between  $42^{nd}$   $Na^+$  ion and a set of oxygen atoms over period of transition for simulation 3. The  $42^{nd}$   $Na^+$  ion approximately moves from the  $O62$  atom on the third residue of the third chain to the  $O62$  atom on the third residue of the first chain in the time period of around 710 ps to 740 ps.

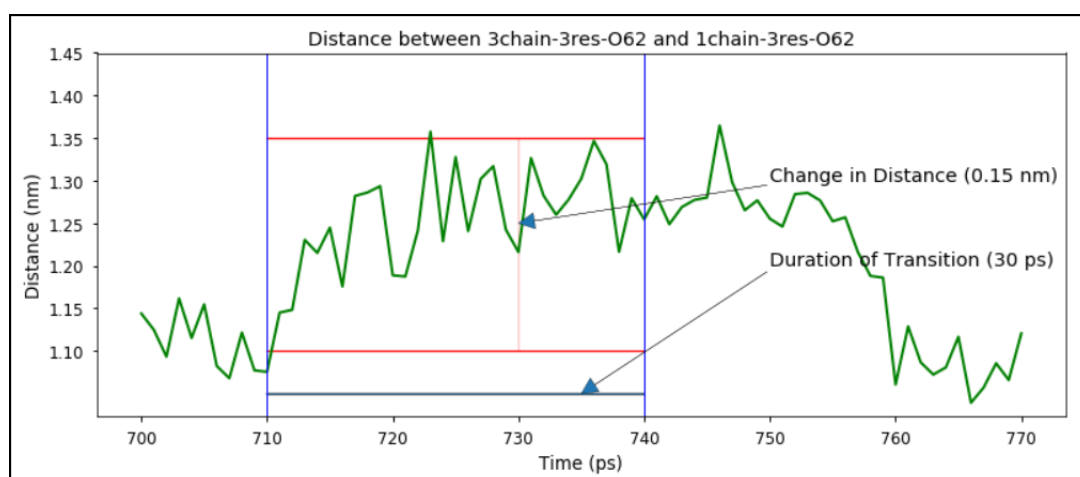


Figure 4.12: Distance between  $O62$  atom on the third residue of the third chain and the  $O62$  atom on the third residue of the first chain remains relatively constant in simulation 3.

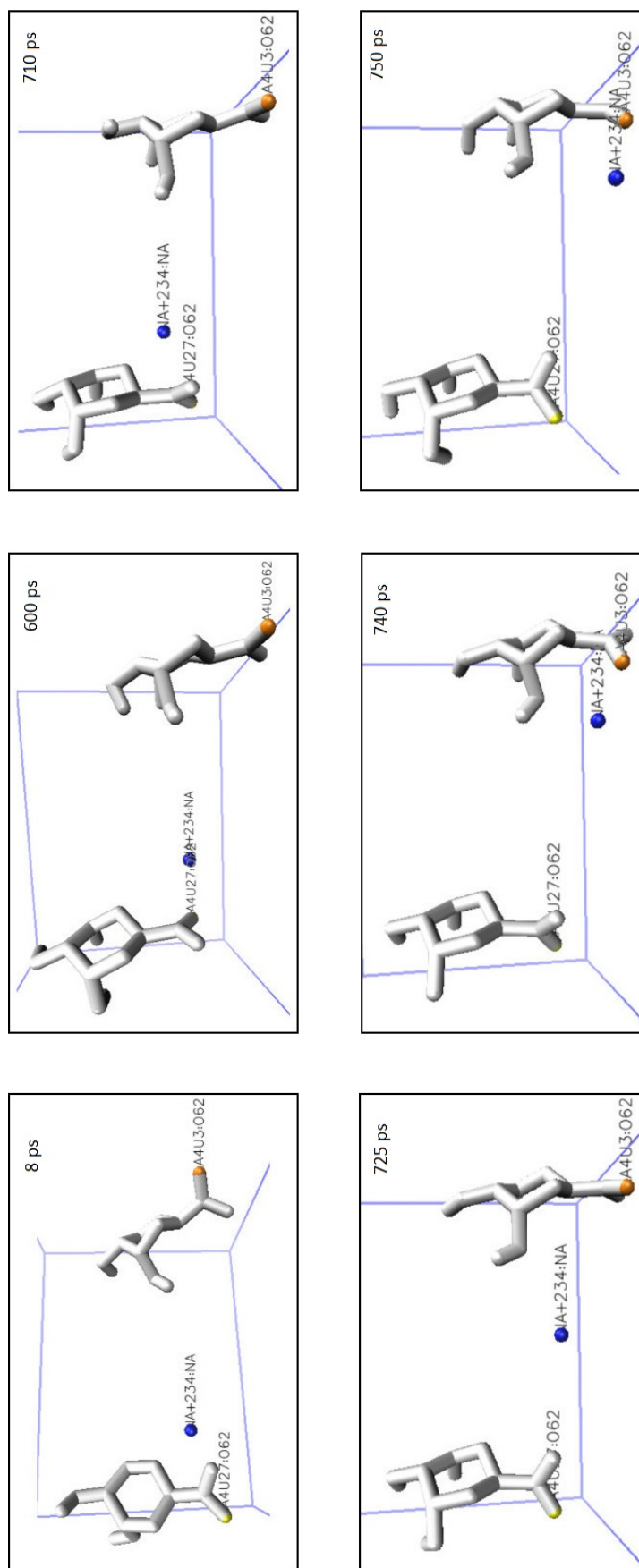


Figure 4.13: Snapshots at progressive time intervals of simulation 3 showing the movement of  $42^{nd}$   $Na^+$  ion from  $O62$  atom (yellow) of one residue to  $O62$  atom (orange) of another residue. In the inset of each image is the time at which the snapshot was taken. Blue lines in the background indicate the rectangular periodic boundary. The  $Na^+$  ion approximately moves from the  $O62$  atom on the third residue of the third chain to the  $O61$  atom on the third residue of the first chain in the duration of around 710  $ps$  to 740  $ps$  [5].

### 4.3. Analysis of the Diffusion Constant

The diffusion constant is calculated using the *diffus* tool specified in Section 3.3.3. The ion diffusion constant is calculated in the three-dimensional ( $D_{xyz}$ ), longitudinal ( $D_z$ ) and transverse ( $D_{xy}$ ) direction.

From Table 4.2, it is clear that the diffusion of any type of ion is pronounced in the transverse ( $D_{xy}$ ) direction rather than the longitudinal ( $D_z$ ) direction. This appears to have been contributed to by the fact that the ions have preferential interaction with  $O_2$  atom.

Table 4.2: The diffusion coefficients are calculated from a linear least-square fit of mean square displacements over the time-period 0 to 3 ns, each of them calculated over the entire simulation period of 10 ns considering all time-origins. The ionic diffusion can be three-dimensional ( $D_{xyz}$ ) or transverse ( $D_{xy}$ ) or longitudinal ( $D_z$ ) and is averaged over all ions of its type. The error estimate is given by the standard deviation divided by square root of the number of ions as shown in parentheses. [2]

Temperature (K)	Simulation	$Ca^{2+}$ (%)	Ion	$D_{xyz}$ ( $10^{-7} cm^2 s^{-1}$ )	$D_{xy}$ ( $10^{-7} cm^2 s^{-1}$ )	$D_z$ ( $10^{-7} cm^2 s^{-1}$ )
300	192 $Na^+$ ions	0	$Na^+$	0.6 (0.07)	0.37 (0.0054)	0.23 (0.0016)
	168 $Na^+$ ions 12 $Ca^{2+}$ ions	6.67	$Na^+$	0.51 (0.0064)	0.32(0.0047)	0.2 (0.0018)
			$Ca^{2+}$	0.24 (0.021)	0.14 (0.0134)	0.1 (0.0083)
	144 $Na^+$ ions 24 $Ca^{2+}$ ions	14.29	$Na^+$	0.31 (0.0064)	0.2 (0.0038)	0.11 (0.0026)
			$Ca^{2+}$	0.14 (0.0091)	0.11 (0.0066)	0.04 (0.003)
	373	192 $Na^+$ ions	0	$Na^+$	2.15 (0.262)	1.41 (0.1744)
168 $Na^+$ ions 12 $Ca^{2+}$ ions		6.67	$Na^+$	2.04 (0.0031)	1.24 (0.1573)	0.8 (0.0022)
			$Ca^{2+}$	0.92 (0.0134)	0.54 (0.0063)	0.38 (0.0075)
144 $Na^+$ ions 24 $Ca^{2+}$ ions		14.29	$Na^+$	1.75 (0.0085)	1.11 (0.0065)	0.64 (0.0022)
			$Ca^{2+}$	0.97 (0.0071)	0.62 (0.0068)	0.35 (0.0025)

The diffusion constant of  $Na^+$  ion drops by around 48% as  $Ca^{2+}$  ion concentration increases to 14.29% at 300 K as shown in Fig. 4.14. A similar trend is observed at 373 K.

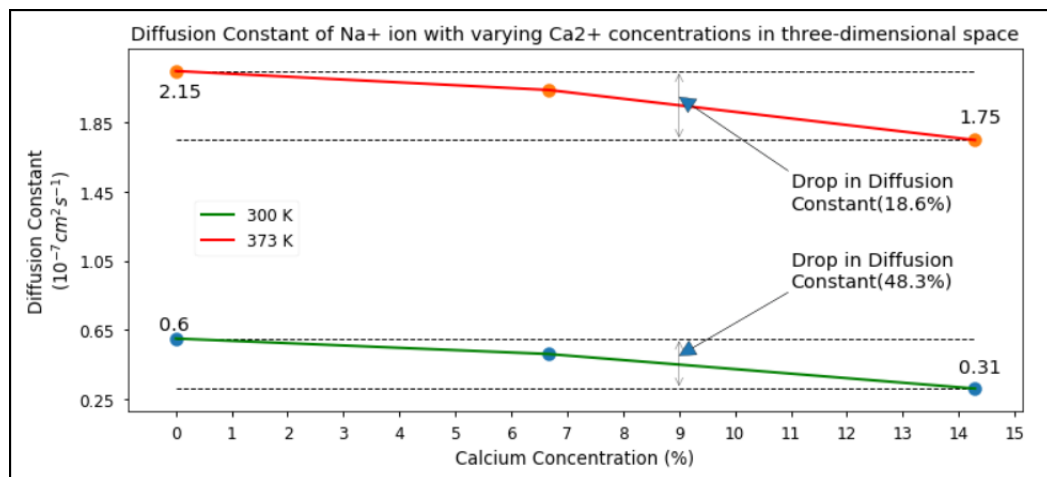


Figure 4.14: At 300 K, the diffusion constant of  $Na^+$  ion drops by around 48% as  $Ca^{2+}$  ion concentration increases to 14.29%. At 373 K, the diffusion constant of  $Na^+$  ion drops by around 18.3% as  $Ca^{2+}$  ion concentration increases to 14.29%.

The observed diffusion constant can be compared with the diffusion constant calculated in [6] as shown in Table 4.3. In general, the diffusion constant at 373 K is calculated to be higher than those of Lithium ion in [6].

Table 4.3: Diffusion Constant calculated for PEO (Polyethylene Oxide) system in [6] is compared with the sodium alginate system under analysis at 373 K

<b>PEO System</b>	<b>Ion</b>	<b>Diffusion Constant (<math>10^{-7}cm^2s^{-1}</math>)</b>	<b>Sodium Alginate System</b>	<b>Ion</b>	<b>Diffusion Constant (<math>10^{-7}cm^2s^{-1}</math>)</b>
$P(EO)_8 - LiClO_4$	$Li^+$	0.16	144 $Na^+$ ions 24 $Ca^{2+}$ ions	$Na^+$	1.75
$P(EO)_{16} - LiClO_4$	$Li^+$	0.32	168 $Na^+$ ions 12 $Ca^{2+}$ ions	$Na^+$	2.04
$P(EO)_{31} - LiClO_4$	$Li^+$	2.02	192 $Na^+$ ions	$Na^+$	2.15

# 5

## Conclusions and Recommendations

*Building on the methodology of simulation creation and analysis in Chapter 3, the outcomes were analyzed in depth in Chapter 4. Using this information, the research question that forms the scope of the thesis, mentioned in Chapter 1 can be answered comprehensively.*

*Section 5.1 draws upon the knowledge gained from chapters 1 to 4 to detail key findings. Section 5.2 establishes recommendations for future research and for carrying forward the work done here in application for other electrolyte systems.*

### 5.1. Conclusions

The purpose of this project was to study the feasibility of alginate as polymer electrolyte through molecular dynamics simulations. 16 alginate chains were inserted in a rectangular periodic box and  $Na^+$  &  $Ca^{2+}$  ions were added to neutralize. Multiple simulations were run at varying concentrations of  $Ca^{2+}$  ions. MD Simulations to understand polymer electrolyte mechanism were done for the first time at the Storage of Electrochemical Energy Department. The guluronate residue is shown in Fig. 5.1 to aid the explanation of the conclusions.

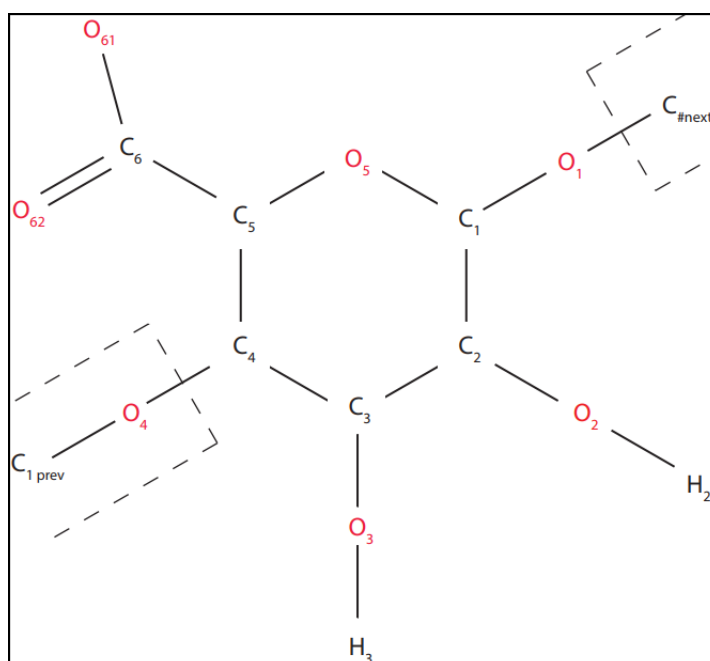


Figure 5.1: Guluronate residue with the different oxygen atoms.

The main conclusions of this project are listed below:

- $Na^+$  ion can hop from one location to another in sodium alginate polymer electrolytes. This is evidenced by local small scale movement of an arbitrary  $Na^+$  ion from the vicinity of oxygen atom of one residue to the vicinity of another oxygen atom on another residue. The transition happens over a time-period of about 30 *ps*. The  $Na^+$  ion moves about 0.8 *nm* while the change in distance between oxygen atoms is only 0.15 *nm*.
- Diffusion constant drops by 48% with the addition of  $Ca^{2+}$  ions while increasing  $Ca^{2+}$  ion concentration to 14.29% at 300 K. However, it is still high enough to be considered as a suitable candidate for solid-state polymer electrolytes. The drop in diffusion constant (18.6%) is much lesser at a higher temperature of 373 K.
- $Na^+$  ion preferentially interacts with O2 atom of the guluronate residue compared to O61 and O62 as the distance between the most likely  $Na^+$  ion - Oxygen bond is larger than the distance between O61 and O62 leading to spreading of charge influence.
- $Na^+$  ion preferentially interacts with O2 atom of the guluronate residue compared to O3 atom as the O2 atom's electronegativity is more pronounced due to its involvement in larger number of hydrogen bonds than O3. The larger involvement in hydrogen bonds appears to arise from the polyguluronate structure itself.
- The diffusion constant at 373 K is approximately 4 times that at 300 K with slight variations depending on the concentration of  $Ca^{2+}$  ion.
- The development of a comprehensive manual for establishing MD simulations for polymer electrolytes.

The above also answer the research questions that the project initially started with 1. The following section deals with recommendations that can be incorporated for future work.

## 5.2. Future Work

Although this project proved the potential of using GROMOS MD simulation for understanding the mechanism of alginate as a polymer electrolyte, it has certain limitations that can be addressed for strengthening the analysis. Following are the recommendations that can be incorporated in future work:

1. Alginates are primarily made of mannuronate and guluronate residues. This project focussed only on guluronate residues. A comprehensive analysis can be done when taking into account both the residues. Different concentrations of these residues can be simulated to understand their effect on the diffusion of  $Na^+$  ion. Analysis can be done to understand if there is any change in the interactions involved with the  $Na^+$  ion. This analysis can guide the desired ratio of mannuronate to guluronate residues for an optimized functioning of a polymer electrolyte during experiments.
2. Real-world polymer electrolytes almost certainly contain plasticizers to provide mechanical flexibility and good surfacial contact with electrodes. Different plasticizers such as glycerol can be inserted in the MD simulation to understand their impact on all of the described processes. Careful analysis can guide the amount of plasticizer that is ideal without a large drop in diffusion or conductivity of  $Na^+$  ion while preserving the favourable characteristics of it.
3. In reality, alginate chains are found to be made of at least 40 residues [2] and are most likely unrestricted in movement. The current project restricts movement in the z-direction by making the chains infinite in length. It will be of interest to find out if there is any change in behavior of the chains. Ideal chain length can be found and efforts could be made to synthesize alginates of corresponding length for experiments.
4. Neutron Magnetic Resonance can be conducted on prepared samples to validate the outcomes of the MD simulations. Diffusion constant can be determined through NMR tests on pure sodium alginate and compared with results from the MD simulation.



# A manual for molecular dynamics implementation and analysis of polymer electrolytes with GROMOS

This manual contains an explanation on how to set up molecular dynamics simulations for polymer electrolytes on GROMOS96 program.

In order to observe the dynamics of molecules of polymer electrolyte, and analyze the results of the same, certain steps need to be followed. These are outlined in this chapter. Section [A.1](#) outlines the step-wise implementation of the molecular dynamics simulation. Section [A.2](#) to Section [A.8](#) explain in detail the different stages leading to molecular dynamics.

We used GROMOS as the software to implement molecular dynamics simulation because:

- It has great documentation.
- It is significantly faster than time-consuming quantum mechanics based simulations for polymers that contain large number of atoms.
- Existing literature or prior-art on alginate molecular dynamics simulation.

## A.1. Step-Wise Implementation

Firstly, the directory structure specified as shown in Fig. [A.1](#). This is done by creating a location in the UNIX workspace (available within the Sustainable Electrochemical Energy (SEE) group) which is accessible to GROMOS and executing the command below:

```
unzip alginate_multiple_chains.zip
```

All steps henceforth aim to establish a 16-chain alginate polymer placed end-to-end in a periodic rectangular box with 192 positive ions for neutralization. Each chain consists of 12 residues and 12 negative charges due to oxygen anions. 168 sodium ions and 12 calcium ions are used for neutralization. The following stages are executed sequentially:

### 1. Topology Generation

Topology generation is carried out in **topo** directory. Input files required are:

```
45a4_mod.mtb  45a4.ifp  make_top_alginate.arg  com_top_alginate.arg  
com_top_alginate_NA.arg  com_top_alginate_NA_CA.arg  
check_top_alginate_NA_CA.arg  45a4.mtb  45a4_carbo.mtb
```

The ions and the polymer required are decided before-hand. Their definitions are copied into **45a4\_mod.mtb** from **45a4.mtb** and **45a4\_carbo.mtb**.



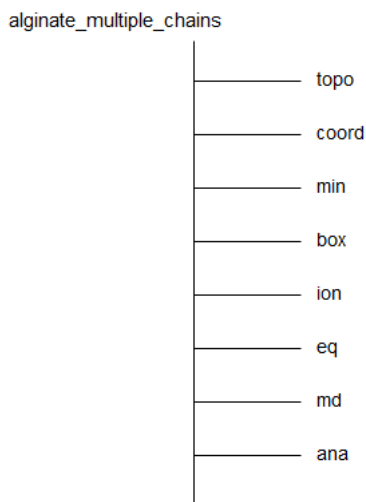


Figure A.1: Working Directory Structure for Molecular Dynamics in GROMOS.

The topology file for a single-chain polymer is generated using below command. If a different polymer is desired, refer Section [A.2.1](#).

```
make_top @f make_top_alginate.arg > alginate.top
```

The topology file for any ion X can be generated by copying and modifying **make\_top\_X.arg**. This is explained further in Section [A.2.2](#).

```
make_top @f make_top_NA.arg > NA_45a4.top
make_top @f make_top_CA.arg > CA_45a4.top
```

The chains are combined by executing the following command; refer Section [A.2.3](#) for more information.

```
com_top @f com_top_alginate.arg > alginate_multiple.top
```

The solute is combined with ions using the below commands, followed by a final check for inconsistency which is also explained in Section [A.2.3](#).

```
com_top @f com_top_alginate_NA.arg > alginate_multiple_NA.top
com_top @f com_top_alginate_NA_CA.arg > alginate_multiple_NA_CA.top
check_top @f check_top_alginate_NA_CA.arg > check
```

## 2. Co-ordinate Generation

Co-ordinate generation is carried out in **coord** directory. The input files needed are:

```
pdb2g96_alginate.arg  pdb2g96.lib  gch_alginate.arg
alginate.pdb
```

For a single chain, the following command is executed. For more than one chain, refer Section [A.3.1](#).

```
pdb2g96 @f pdb2g96_alginate.arg > pdb2g96_alginate.cnf
```

Hydrogen atoms co-ordinates are reassigned based on geometric means using the following command:

```
gch @f gch_alginate.arg > gch_alginate.cnf
```

### 3. Minimization of the solute

Minimization of solute is carried out in **min** directory. The settings are specified in **em\_alginate.imd** and can be modified as required, mentioned in Section A.4. **em\_alginate.run** is modified as mentioned in Section A.4.1 and the minimization stage is executed by the following command:

```
./em_alginate.run
```

### 4. Solvation of the solute

Solvation of the solute is carried out in **box** directory. The input files required are:

```
sim_box_alginate.arg  spc.cnf  em_solvent.run
```

First, the solute from the minimization stage is solvated with water using settings specified in **sim\_box\_alginate.arg**. These settings can be changed by referring Section A.5.1. The following command is executed for solvation:

```
sim_box @f sim_box_alginate.arg > sim_box_alginate.cnf
```

**sim\_box\_alginate.cnf** is copied as **sim\_box\_alginate.por** and **sim\_box\_alginate.rpr**. These two files are modified as given in Section A.5.1. Finally, an energy minimization is carried out on the solute-solvent structure by executing the following. The settings for this command is specified in **em\_solvent.imd** and **em\_solvent.run** needs to be modified as mentioned in Section A.5.2.

```
./em_solvent.run
```

### 5. Ionization for neutralization

Ionization for neutralization is carried out in the **ion** directory. The input files required are:

```
ion_alginate.arg
```

For a single chain, neutralization can be carried out by specifying the number and type of ions required in **ion\_alginate.arg** and executing the following command as mentioned in Section A.6.

```
ion @f ion_alginate.arg > alginate_ion.cnf
```

However, for high density structures, as in the case of multiple chains, external means such as javascripts are used to generate the requisite configuration as mentioned in Section A.6.

### 6. Equilibration of molecular system

Equilibration of the system is carried out in **eq** directory. The settings needed are specified in **equilibration.imd** and can be modified as needed, by referring Section A.7. **eq\_mk\_script.arg** needs to be modified as mentioned in Section A.7.1. At first, the required number of scripts corresponding to temperatures at which the simulation runs are generated using the following command:

```
mk_script @f eq_mk_script.arg
```

Finally, the following command is executed to run the above generated scripts sequentially.

```
./run.csh
```

## 7. Molecular Dynamics

Molecular Dynamics simulation is carried out in **md** directory. The settings needed are specified in **md.imd** and can be modified as needed, by referring Section A.8. **md\_mk\_script.arg** needs to be modified as mentioned in Section A.8.1. At first, ten scripts are generated, each that run the simulation for 1 ns using the following command:

```
mk_script @ md_mk_script.arg
```

Finally, the following command is executed to run the above generated scripts sequentially.

```
./run.csh
```

## 8. Analysis of the Simulation

Following sections detail each of the above stages.

### A.2. Topology Generation

The first stage is the building of a molecular topology file and occurs in the **topo** directory. This file contains force-field data concerning the polymer molecule at study. Three files are necessary for the creation of a topology file:

#### 1. Molecular topology building blocks (.mtb):

These contain specific information (dihedral angles between atoms, atoms and their order, bond angles) of various residues of solutes and solvents. A residue is equivalent to a monomer of the polymer. All .mtb files must be combined into one file (Here, 45a4.mtb containing the ions was combined with 45a4\_carbo.mtb containing the polymer residues to form 45a4\_mod.mtb).

#### 2. Interaction function parameter file (.ifp):

It is an exhaustive detailed list of interactions between all types of atoms that the .mtb files refer to.

#### 3. Argument file (.arg):

It contains information on the arrangement of the different residues in the solute, whether the residues need to be connected cyclically, the type of solvent needed, the interaction parameter file and molecular topology building block files to be used.

In the topology generation stage, the following commands are executed sequentially:

```
make_top @f make_top_alginate.arg > alginate.top
make_top @f make_top_NA.arg > NA_45a4.top
make_top @f make_top_CA.arg > CA_45a4.top
com_top @f com_top_alginate.arg > alginate_multiple.top
com_top @f com_top_alginate_NA.arg > alginate_multiple_NA.top
com_top @f com_top_alginate_NA_CA.arg > alginate_multiple_NA_CA.top
check_top @f check_top_alginate_NA_CA.arg > check
```

Each of the downstream stages need a unique topology file as ions, solvent and if any other structure required are inserted stage-wise. Below are the stages where a unique topology file is needed:

#### 1. Coordinate Generation:

The topology file should contain only the solute and solvent as here, only the solute or the polymer chain gets created. This remains until the Ionization stage is reached.

## 2. Ionization for neutralization:

In this stage, in addition to the solute and solvent, ions are inserted. Hence, a dedicated topology file consisting the solute and ions is needed. If there are multiple types of ions, there may be a need to have corresponding topology files.

Each of the commands listed in [A.2](#) are explained in detail below:

### A.2.1. `make_top @f make_top_alginate.arg > alginate.top`

This command creates the topology file which contains the connections between atoms and monomer units along with interactions between the various atoms involved in the solute/polymer chain and that of the solvent.

```
# specify which forcefield building blocks and parameters you want to use
# with the @build and @param arguments.
@build 45a4_mod.mtb
@param 45a4.ifp
# using the @seq argument you tell the program which building blocks you
# want to put in a row to built your peptide.
@seq    cyclic kA4U kA4U kA4U kA4U kA4U kA4U kA4U kA4U kA4U kA4U kA4U kA4U
# Specify the solvent.
@solv   H2O
```

The file **make\_top\_alginate.arg** shown above contains:

#### 1. **@build:**

To specify the molecular topology building block file to use (Here, `45a4_mod.mtb`<sup>1</sup>).

#### 2. **@param:**

To specify the interaction function parameter file to use (Here, `45a4.ifp`).

#### 3. **@seq:**

To specify the sequence of monomer units. Monomer units need to be specified as a code given in the `.mtb` file. (Here, `kA4U` represents 4-L-gulonate-alpha-1 residue). `cyclic` is appended at the beginning if it needs to be specified as a continuous polymer chain (Here, a cyclic sequence of 4-L-gulonate-alpha-1 residues is specified).

#### 4. **@solv:**

To specify the solvent (Here,  $H_2O$ ).

### A.2.2. `make_top @f make_top_NA.arg > NA_45a4.top`

This command generates a topology file **NA\_45a4.top** containing only sodium ions.

The file **make\_top\_NA.arg** differs from the file **make\_top\_alginate.arg** in the **@seq** parameter which is set to `NA+`.

If other ions are needed in the molecular dynamics framework, a similar file can be generated and executed by changing the `@seq` parameter to the corresponding ion. In this case, apart from sodium ions, calcium ions are also inserted. Hence, the command below is also executed:

```
make_top @f make_top_CA.arg > CA_45a4.top
```

Now, all the required topology files are generated. However, they need to be combined appropriately to be suitable for the downstream stages. This is discussed in the following sections.

<sup>1</sup>45a4 refers to the force-field version in GROMOS. GROMOS regularly releases updates on force-fields.

**A.2.3. com\_top @f com\_top\_alginate.arg > alginate\_multiple.top**

This command creates 16 copies of **alginate.top** and combines them into a single solute to form **alginate\_multiple.top**.

```
# this combines several topologies into one solute topology.
@topo 16:alginate.top
# the parameters (what you specified with @param in maketop) are taken from
# the first topology.
@param 1
# the solvent is taken from the first topology.
@solv 1
```

The file **com\_top\_alginate.arg** shown above contains:

**1. @topo:**

Various combinations and multiples of different generated topology files can be specified (Here, 16 chains of 12-residue alginate are combine).

**2. @param:**

1 specified implies that the interaction function parameter file is taken from the first topology file mentioned in @topo.

**3. @solv:**

1 specified implies that the solvent is taken from the first topology file mentioned.

```
# this combines several topologies into one solute topology.
@topo 1:alginate_multiple.top 168:NA_45a4.top
# the parameters (what you specified with @param in maketop) are taken from
# the first topology.
@param 1
# the solvent is taken from the first topology.
@solv 1
```

Similarly, **com\_top\_alginate\_NA.arg** shown above can be used to combine **alginate\_multiple.top** and **NA\_45a4.top** into **alginate\_multiple\_NA.top**.

Similarly, **com\_top\_alginate\_NA\_CA.arg** can be used to combine the **alginate\_multiple.top**, **NA\_45a4.top** and **CA\_45a4.top** into **alginate\_multiple\_NA\_CA.top**.

Care should be taken to ensure the total amount of negative charges is balanced by total amount of positive charge for neutrality.

```
Each alginate chain has 12 negative charges
Total negative charges = 12 X 16 chains = 192 negative charges
For neutralization,
168 Na+ ions and 12 Ca2+ ions = 192 positive charges
```

A final **check\_top** command can be run to ensure no inconsistencies exist in the final **alginate\_multiple\_NA\_CA.top** file.

```
check_top @f check_top_alginate_NA_CA.arg > check
```

For this, **check\_top\_alginate\_NA\_CA.arg** file is shown below:

```
# check_top performs a check of the topology file. Give it with the @topo
# argument.
@topo com_top_alginate_NA_CA.top
# add the forcefield building block and parameter arguments to do a more
# careful check against the force-field.
@build 45a4_mod.mtb
@param 45a4.ifp
```

At the end of this stage these files generated will be used for the following stages:

```
alginate_multiple.top
alginate_multiple_NA.top
alginate_multiple_NA_CA.top
```

### A.3. Co-ordinate Generation

Once all the topology files are generated, the physical location of each atom needs to be specified and this is done in **coord** directory. Co-ordinate file generations is done by executing the following commands which are also discussed in detail subsequently:

```
pdb2g96 @f pdb2g96_alginate.arg > pdb2g96_alginate.cnf
gch @f gch_alginate.arg > gch_alginate.cnf
```

#### A.3.1. pdb2g96 @f pdb2g96\_alginate.arg > pdb2g96\_alginate.cnf

For a single chain, the co-ordinate generation process is straightforward. A corresponding protein data bank (.pdb) file representing the physical locations and connections for the 12-residue polyguluronate chain was downloaded from London South Bank University[1]. The file **pdb2g96\_alginate.arg** shown below uses the topology information created in the previous stage and combines it with the physical .pdb information to generate a configuration (.cnf) file.

```
@topo ../topo/alginate.top
# the PDB file you want to convert
@pdb alginate.pdb
@lib pdb2g96.lib
```

The following command is executed to generate a configuration file for a single chain.

```
pdb2g96 @f pdb2g96_alginate.arg > pdb2g96_alginate.cnf
```

However, if there is a need to generate the physical location of multiple chains, the above procedure cannot be followed due to the lack of appropriate .pdb file. Instead, the configuration file generated from a single chain can be modified and new chains can be inserted with translated co-ordinates of the original chain.

For this purpose, a JAVA script was written that parses through the original configuration file and prints out the modified configuration file. The **java\_files** directory under coord directory contains all the files related to this. The file **pdb2g96\_alginate.cnf** is renamed to **alginate.cnf** and copied to **java\_files**.

The settings that need to be passed in to ChainReader.java are specified below:

```

* res_add      - last residue in the input file / number of residues that
* will be added in the output file
* atom_add     - last atom in the input file / number of atoms that will be
* added in the output file
* x_dist_add   - distance by which the x co-ordinate is translated by
* y_dist_add   - distance by which the y co-ordinate is translated by
* input_file   - alginate_NUM.cnf, where NUM represents number of chains
* output_file  - specify name of output file
*
* output_file  > res_add, atom_add, x_dist_add, y_dist_add, input_file
* alginate_2.cnf > 12,      168,      0.7,      0.0,      alginate.cnf
* alginate_4.cnf > 24,      336,      1.7,      0.0,      alginate_2.cnf
* alginate_8.cnf > 48,      672,      0.0,      1.0,      alginate_4.cnf
* alginate_16.cnf > 96,     1344,     0.0,      2.0,      alginate_8.cnf

```

Following are the steps to generate a 16 alginate chain polymer with verification:

```

Step 1 - Use settings specified above appropriately to run ChainReader.java
Step 2 - Use frameout command to generate a pdb that can be visualized
Step 3 - View pdb and verify if the distances and atoms generated are
        satisfactory. If not, modify the input configuration file and
        restart from Step 1
Run the above steps iteratively, until 16 chains are observed.

```

**ChainReader.java** file is executed iteratively to generate **alginate\_2.cnf**, **alginate\_4.cnf**, **alginate\_8.cnf** and **alginate\_16.cnf**. The flowchart for this process is shown in Fig. A.2.

The command **frameout** is used to generate a **.pdb** file from the **.cnf** file. This is helpful for visualization. Another consideration while using **frameout** is to use the topology file that corresponds to the chains present in the configuration file. **frameout** is executed on **frameout\_alginate.arg** file which contains the following fields that need to be modified accordingly:

```

@topo ../topo/alginate_multiple.top
@pbc      r 7
@outformat pdb
@notimeblock
@traj     alginate_16.cnf

```

Once **alginate\_16.cnf** is generated, it is renamed to **pdb2g96\_alginate.cnf**. The size of the rectangular periodic box is appended at the end of this file. Care should be taken to provide dimension size at least more than two times greater than the minimum long-distance range for reaction field cut-off radius (1.4 nm as specified in the energy minimization stage). Also, it was desired to create an infinitely long chain in the z-direction. Hence, the z-dimension of the rectangular box specified is minimally greater than the length of the polymer chain. This specification takes advantage of the rectangular periodic boundary conditions. This is shown below.

```

# The second row of GENBOX represents the dimensions of the box in x, y and
# z directions while the third row represents the 90 degree angles as
# the box is rectangular - all distances are in nm
GENBOX
1
3.800000000    2.900000000    5.250000000
90.000000000  90.000000000  90.000000000
0.000000000    0.000000000    0.000000000
0.000000000    0.000000000    0.000000000
END

```

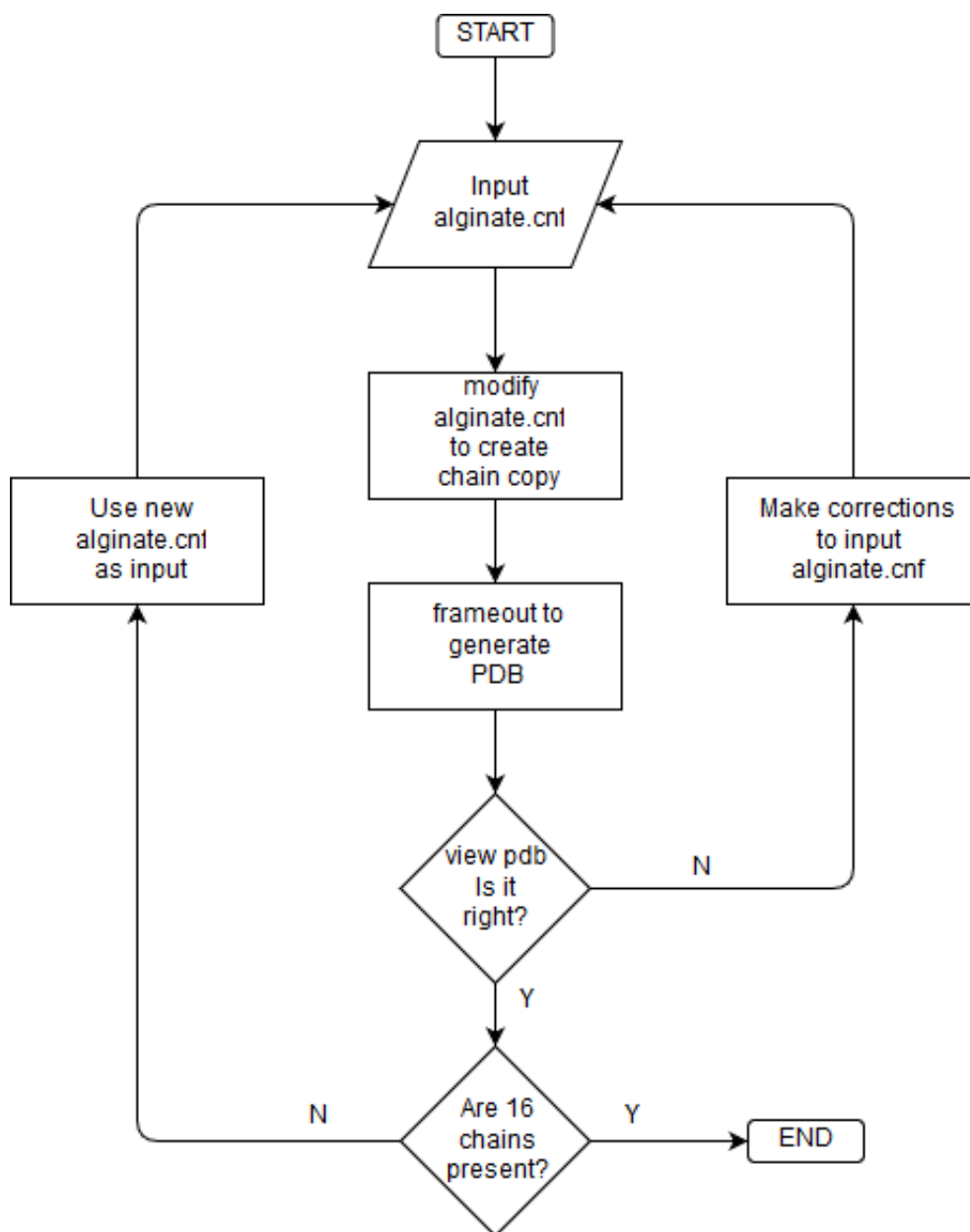


Figure A.2: The process of generation of required number of alginate chains.

### A.3.2. `gch @f gch_alginate.arg > gch_alginate.cnf`

`gch` command reassigns co-ordinates of all the hydrogen atoms based on geometric means.

```
gch @f gch_alginate.arg > gch_alginate.cnf
```

The file **gch\_alginate.arg** contains the following fields that need to be modified accordingly:



```
@topo ../topo/alginate_multiple.top
# the coordinates from which you want to generate the hydrogens
@pos pdb2g96_alginate.cnf
# All hydrogens within a bond length tolerance of 0.1\% are kept
# - the others are generated
@tol 0.1
# Specify rectangular periodic boundary conditions
@pbc r
```

## A.4. Minimization of the Solute

Minimization of the solute is done in the **min** directory by executing the following command:

```
./em_alginate.run
```

Minimization is done to keep the net inter-atomic force on any atom close to zero. This relaxation of energy is necessary to ensure there are no extremely large forces acting in the production stage of molecular dynamics. Extremely large forces can lead to errors and crashing of the simulation. For energy minimization certain parameters need to be specified. These are provided in the **em\_alginate.imd** file. The main changes to this file are:

1. **NSTLIM** in **STEP** block:

The number of steps energy minimization has to run for, to ensure most possible minimization. If the number of steps specified is large enough, the GROMOS engine automatically carries out the necessary number of steps only.

2. **DT** in **STEP** block:

A time-step of 2 fs is specified.

3. **NTB** in **BOUNDCOND** block:

NTB 1 defines rectangular periodic boundary condition simulation. This is required as we are simulating a polymer structure that needs to be infinite in all directions. Other settings such as vacuum or octahedral boundary conditions are specified in the GROMOS Manual.

4. **NDFMIN** in **BOUNDCOND** block:

NDFMIN 3 specifies 3 degrees of freedom that must be subtracted from total degrees of freedom for the calculation of temperature.

5. **NTCP** and **NTCS** in **CONSTRAINT** block:

These are set to 1 to specify the usage of SHAKE algorithm to constrain solute and solvent bonds respectively.

6. **NTCP0** and **NTCS0** in **CONSTRAINT** block:

A geometric tolerance of  $10^{-4}$  is specified to constrain all bond lengths.

7. **NTC** in **CONSTRAINT** block:

This is set to 3 to specify that constraints are applied for both solute and solvent bonds.

8. **NRE(1)** in **FORCE** block:

This represents the last atom in the energy group of the solute. For 16 chains of 12-residue polyguluronate, this number turns out to be 2688.

9. **RCUTP** and **RCUTL** in **PAIRLIST** block:

These are set to 0.8 nm and 1.4 nm to specify short-range and long-range cut-off distances respectively in pairlist creation.

#### 10. **NSNB** in **PAIRLIST** block:

A frequency of 5 steps for updating the short-range pairlist and immediate-range interactions is specified.

#### 11. **EPSRF** in **NONBONDED** block:

A relative dielectric permittivity of 1 is specified as a polymer electrolyte is an anhydrous medium.

### A.4.1. `./em_alginate.run`

**em\_alginate.run** contains the following fields that need to be modified accordingly:

```
#!/bin/sh
GROMOS=md
$GROMOS \
# topology file corresponds to that of the solute or the 16 chain polymer
@topo ../topo/alginate_multiple.top \
# configuration file to be specified is generated in the previous stage
@conf ../coord/gch_alginate.cnf \
# name of output configuration file
@fin  alginate_min.cnf \
# input parameters for minimization are specified in em_alginate.imd
# output file is present in em_alginate.omd
@input em_alginate.imd > em_alginate.omd
```

**em\_alginate.omd** must be examined to ensure that there were no errors during energy minimization process. The most common errors are SHAKE errors. These happen due to placement of atoms closer than normal or if one atom was over another. The SHAKE algorithm is unable to constrain the bond lengths due to large forces. One example where SHAKE was encountered was when the z-dimension was not large enough to allow for an infinite polymer chain. This led to atoms at the end of the chain being too close. This error was fixed by increasing the value of z-dimension.

## A.5. Solvation of the solute

In real conditions of any peptide or protein compound, the solute is always surrounded by some kind of solvent. However, for the case of polymer electrolyte molecular dynamics, especially Lithium-ion or Sodium-ion batteries, environments are anhydrous. Therefore, we will solvate the solute and retain only the number of solvents as the number of ions required for neutralization. This is because in the following stage, all solvent molecules are replaced by positive ions. Solvation of the solute is done in **box** directory. This stage consists of two important sub-stages:

1. Initialization of solvent molecules
2. Minimization of the solvent-solute structure

The following commands are executed in the minimization stage and are explained in detail below:

```
sim_box @f sim_box_alginate.arg > sim_box_alginate.cnf
./em_solvent.run
```

### A.5.1. `sim_box @f sim_box_alginate.arg > sim_box_alginate.cnf`

This sub-stage initializes the solvent molecules. The solvent (here,  $H_2O$ ) is a pre-equilibrated box of water molecules of fixed dimensions. Two considerations need to be taken care of here:

1. The box size of the solvated polymer can be taken from the original polymer box size from the previous stage. This can be specified by using **@boxsize** specified below. The box size can also be recreated by specifying the distance of the polymer from the wall in all three dimensions. This is done using **@minwall** option shown below.

- The minimum distance between solute and solvent is specified using **@thresh**. Here, 0.23 nm is specified.

The arguments present in the **sim\_box\_alginate.arg** file need to be modified accordingly:

```
@topo    ../topo/alginate_multiple.top
# We use a cubic box (r = rectangular)
@pbc     r
# coordinates of the solute.
@pos     ../min/alginate_min.cnf
# coordinates of the box containing SPC water molecules.
@solvent spc.cnf
# the minimum solute-wall distance
# @minwall 2.37 2.15 0.0
# the minimum solute-solvent distance
@thresh  0.23
# used if one uses truncated octahedron pbc
# @rotate
# @gather
@boxsize
```

Once **sim\_box\_alginate.cnf** is generated, only 180 solvent molecules are retained, while the rest are deleted as shown in Fig. A.3. **sim\_box\_alginate.cnf** is copied as **sim\_box\_alginate.por** and **sim\_box\_alginate.rpr** files as shown in Fig. A.4 and Fig. A.5 respectively. In the **sim\_box\_alginate.por** file or the position restraints file, POSITION is changed to POSRESSPEC, all solvent molecules are removed and the dimension information is deleted. In the **sim\_box\_alginate.rpr** file or the reference positions file, POSITION is replaced by REFPOSITION.

<pre>TITLE Solvating ../min/alginate_min.cnf in spc.cnf Box dimensions (rectangular) were specified by user Added 606 solvent molecules END POSITION 1 kA4U C3      1 -0.591155733 -0.088930310 -0.197794369 1 kA4U O3      2 -0.514086687 -0.108502191 -0.317263168 1 kA4U HO3     3 -0.416177110 -0.113857070 -0.297640725 1 kA4U C2      4 -0.742270243 -0.104582009 -0.202988122 1 kA4U O2      5 -0.812160962 -0.226710049 -0.231135581 1 kA4U HO2     6 -0.754931467 -0.300530007 -0.195417206</pre>	<pre>179 SOLV HW2  3225  1.073498759  0.576925464 -1.520674041 180 SOLV OW  3226  0.308085070  0.563188325 -1.473730006 180 SOLV HW1  3227  0.208966510  0.576431882 -1.475069154 180 SOLV HW2  3228  0.330752607  0.476735165 -1.518603911 END GENBOX 1 3.800000000  2.900000000  5.250000000 90.000000000 90.000000000 90.000000000 0.000000000 -0.000000000 0.000000000 0.000000000 0.000000000 0.000000000 END</pre>
------------------------------------------------------------------------------------------------------------------------------------------------------------------------------------------------------------------------------------------------------------------------------------------------------------------------------------------------------------------------------------------------------------------------------------------------------------------------------------------------------------	--------------------------------------------------------------------------------------------------------------------------------------------------------------------------------------------------------------------------------------------------------------------------------------------------------------------------------------------------------------------------------------------------------------------------

Figure A.3: **sim\_box\_alginate.cnf**

<pre>TITLE solute atoms to be positionally restrained END POSRESSPEC 1 kA4U C3      1 -0.591155733 -0.088930310 -0.197794369 1 kA4U O3      2 -0.514086687 -0.108502191 -0.317263168</pre>	<pre>192 kA4U C5    2684  1.679735559  0.358879687  0.223676243 192 kA4U O5    2685 -1.991147852  0.397298337  0.174227640 192 kA4U C1    2686 -1.969077091  0.533899656  0.136167625 192 kA4U O1    2687 -2.016356080  0.615417174  0.027946361 192 kA4U C4    2688 -1.994930689  0.574533734 -0.107941789 END</pre>
--------------------------------------------------------------------------------------------------------------------------------------------------------------------------------------------	-----------------------------------------------------------------------------------------------------------------------------------------------------------------------------------------------------------------------------------------------------------------------------------------------------------------------

Figure A.4: **sim\_box\_alginate.por**

<pre>TITLE reference positions for restraining solute atoms END REFPOSITION 1 kA4U C3      1 -0.591155733 -0.088930310 -0.197794369 1 kA4U O3      2 -0.514086687 -0.108502191 -0.317263168 1 kA4U HO3     3 -0.416177110 -0.113857070 -0.297640725 1 kA4U C2      4 -0.742270243 -0.104582009 -0.202988122 1 kA4U O2      5 -0.812160962 -0.226710049 -0.231135581 1 kA4U HO2     6 -0.754931467 -0.300530007 -0.195417206</pre>	<pre>180 SOLV HW1  3227  0.208966510  0.576431882 -1.475069154 180 SOLV HW2  3228  0.330752607  0.476735165 -1.518603911 END GENBOX 1 3.800000000  2.900000000  5.250000000 90.000000000 90.000000000 90.000000000 0.000000000 -0.000000000 0.000000000 0.000000000 0.000000000 0.000000000 END</pre>
-----------------------------------------------------------------------------------------------------------------------------------------------------------------------------------------------------------------------------------------------------------------------------------------------------------------------------------------------------------------------------------------------------------------------------------	-------------------------------------------------------------------------------------------------------------------------------------------------------------------------------------------------------------------------------------------------------------------------------------------------------

Figure A.5: **sim\_box\_alginate.rpr**

### A.5.2. ./em\_solvent.run

The second sub-stage consists of minimization of the solute-solvent structure. The parameters required for this minimization are present in **em\_solvent.imd** file:

**1. NSM:**

The number of solvent molecules is set to 180 as there are 180 ions to be inserted in the next stage. The reasoning behind this is given in Section A.6.

**2. NEGR, NRE(1) and NRE(2):**

In the FORCE block, NEGR is set to 2 as there are solute and solvent energy groups. NRE(1) is set to 2688 or the last atom in the solute. NRE(2) is set to 3228 or the last atom of the solvent.

**3. EPSRF:**

Relative dielectric permittivity is set to 61 in the NONBONDED block since water is the solvent [2].

**em\_solvent.run** file contains the following fields which need to be modified accordingly:

```
#!/bin/sh
GROMOS=md
$GROMOS \
# topology file specification
@topo ../topo/alginate_multiple.top \
# non-minimized solute-solvent configuration file
@conf sim_box_alginate.cnf \
# output file for minimized configuration file
@fin alginate_box.cnf \
# reference positions for the minimization process
@refpos sim_box_alginate.rpr \
# position restraints
@posrespec sim_box_alginate.por \
# parameters for the minimization process is in em_solvent.imd
# output of the minimization process is in em_solvent.omb
@input em_solvent.imd > em_solvent.omb
```

The **em\_solvent.omb** file containing the output of the minimization process can be examined for errors.

**A.6. Ionization for neutralization**

```
ion @f ion_alginate.arg > alginate_ion.cnf
```

Ionization is carried out in **ion** directory by running the above command. The file **ion\_alginate.arg** contains the following fields which need to be modified accordingly:

```
@topo      ../topo/alginate_multiple.top
@pbc       r
# the type of ions is specified by @positive or @negative
# the number of ions and the ion is also specified
@positive  168 NA+
# @random is used for random replacement of the solvent molecules
# @potential is another technique used for replacement of solvent molecules
@random    200
# @pos is to refer to the box of minimized solute-solvent configuration
@pos       ../box/alginate_box.cnf
```

When there is high density of atoms in the rectangular box, GROMOS has difficulty in deciding which solvent molecules to replace despite providing the @random mechanism or the @potential mechanism. To overcome this problem, a javascript was written. The script takes a modified **alginate\_box.cnf** as input and produces **alginate\_168NA\_12CA.cnf** file. The javascript is present in the directory **java\_files**. The settings required for this javascript is:

```

* Takes in a list of ions and a corresponding list of number of each of
* them to be inserted
* Outputs a file where solvent molecules are replaced with requested ions
*
* Output          > start_atom, start_res, num_ion_each, ion_list
* Example:
* alginate_ion.cnf > 2688,          192,          {168,12},          {"NA+","CA2+"}
* alginate_ion.cnf > 2688,          192,          {96},             {"MG2+"}

```

The steps for producing the final output configuration file are:

```

Step 1 - Copy TITLE, POSITION and GENBOX blocks from alginate_box.cnf to
         ion_test.cnf
Step 2 - In IonCreator.java, set start_atom as 2688 and start_res as 192,
         last atom and last residue in alginate_box.cnf respectively.
         They form starting values for addition of new ions
Step 3 - Specify the type and number of each type of ions as required
Step 4 - Run IonCreator.java and obtain alginate_X.cnf configuration file
Step 5 - The GROMOS utility gets confused between DOS format file and UNIX
         format file. To remove this confusion, the following is executed
         tr -d '\015' <alginate_ion.cnf > alginate_168NA_12CA.cnf

```

At the end of this stage, a configuration file suitable for any molecular dynamics simulation is created.

## A.7. Equilibration of molecular system

In this stage we slowly heat the system to the simulation temperature. The atoms of the solute are positionally restrained and are slowly loosened up in steps of increasing temperature. This is to ensure no large forces are encountered. If the molecular dynamics simulation ran directly at, say, 300K, the atoms of the molecule may be subjected to extremely large forces that GROMOS will not be able to solve and the simulation may crash. The following commands create the different steps and also run the equilibration sequentially on them.

```

mk_script @f eq_mk_script.arg
./run.csh

```

These are that parameters that need to be modified for the equilibration stage in the **equilibration.imd** file:

### 1. **NTICOM:**

In the INITIALISE block, NTICOM is made 2 to remove both translational and rotational center of mass motion in the starting of every equilibration step.

### 2. **NSTLIM:**

In the STEP block, NSTLIM is set to 16650 to represent 0.8 ns of equilibration.

### 3. **TEMPO:**

In the MULTIBATH block, TEMPO is set to 50 K and in subsequent stages, it is increased to the molecular dynamics simulation temperature.

### 4. **NEGR, NRE(n):**

In the FORCE block, the total number of energy groups is specified as 181 (1 solute of 16 chains, 168 NA<sup>+</sup> ions and 12 CA<sup>2+</sup> ions). Each of these groups' last atom is mentioned.

### 5. **EPSRF:**

The dielectric constant is kept as 1 as there is no solvent involved and all the atoms and ions necessary for simulation are already specified.

**CPOR:**

In the POSITIONRES block, CPOR is set to  $2.5 * 10^4$ .

The equilibration must proceed in multiple steps with each step having a slightly higher temperature than the previous step. Here, there are 7 steps in increments of 50K with loosening of position restraints CPOR. These are mentioned in **equilibration.jobs** file shown below:

```
TITLE
General startup protocol.
heating while loosening the position restraints.
END
JOBSCRIPTS
job_id NTIVEL  TEMPI  TEMP0[1]  TEMP0[2]  COUPLE  NTPOR  CPOR  subdir  run_after
1      1      50.0    50.0     50.0     1       1  2.5E4  .       0
2      0      0.0     100.0   100.0     1       1  2.5E3  .       1
3      0      0.0     150.0   150.0     1       1  2.5E2  .       2
4      0      0.0     200.0   200.0     1       1  2.5E1  .       3
5      0      0.0     250.0   250.0     1       1  2.5E0  .       4
6      0      0.0     300.0   300.0     1       1  2.5E-1 .       5
7      0      0.0     300.0   300.0     1       0  0.000  .       6
END
```

The alginate\_168NA\_12CA.cnf from the ionization stage is copied as alginate\_168NA\_12CA.por and alginate\_12CA.rpr with modifications as done in the box stage in Section A.5.1.

### A.7.1. mk\_script @f eq\_mk\_script.arg

This command utilizes the **eq\_mk\_script.arg** to produce scripts for the 7 steps of equilibration. It contains the following fields that need to be modified accordingly:

```
# prefix added to each of seven scripts generated
@sys eq_alginate
# Location of GROMOS MD simulation
@bin      /home/jheringa/gromos/bin/md_mpi
# Location of directory in which all scripts need to be generated
@dir      /home/santhoshshetty/alginate_multiple_chains/eq
@files
topo ../topo/alginate_multiple_NA_CA.top
input equilibration.imd
coord ../ion/alginate_168NA_12CA.cnf
posresspec alginate_168NA_12CA.por
refpos      alginate_168NA_12CA.rpr
# A library file corresponding to all information required for generation
# of scripts
@template mk_script.lib
@version      md++
# List of steps and the constraints specified
@joblist      equilibration.jobs
```

Once this command is executed, seven scripts are generated. The final parameter file **eq\_alginate\_7.imd** needs to be modified for NSTLIM to 400000 to allow it to run for 0.8 ns simulation. All the others steps run for 0.2 ns.

### A.7.2. ./run.csh

Finally, the equilibration stage is executed by running this command. This file contains module load commands, the directory in which equilibration needs to be executed and the first equilibration step

that has to run. The following six steps run in a sequential manner automatically. Each step generates a final configuration file, a trajectory of co-ordinates, a trajectory of energies, and an output of the equilibration operation.

## A.8. Molecular Dynamics

```
mk_script @f md_mk_script.arg
./run.csh
```

The final molecular dynamics stage consists of the simulation of the entire system. Both the atoms of the solute and the ions have been brought to the requisite 300 K or approximately room temperature. This has ensured there are no large forces acting. For the simulation process the parameters are specified in the **md.imd** file. All the other parameters are retained as before.

- **NSTLIM:**

In the STEP block, NSTLIM is set to 500000 or the equivalent of 1 ns simulation.

### A.8.1. mk\_script @ md\_mk\_script.arg

This command utilizes the md\_mk\_.arg to produce scripts for 10 stages of molecular dynamics each about 1 ns. It contains the following fields that need to be modified accordingly:

```
@sys md_alginate
@bin          /home/jheringa/gromos/bin/md_mpi
@dir          /home/santhoshshetty/alginate_multiple_chains/md
@files
  topo ../topo/alginate_multiple_NA_CA.top
  input md.imd
  coord ../eq_settings/eq_alginate_7.cnf
@template mk_script.lib
@version md++
@script 1 10
```

Once this command is executed, ten scripts are generated which each run for 1 ns.

### A.8.2. ./run.csh

The molecular dynamics stage is executed by running this command. This file contains module load commands, the directory in which the simulation needs to be executed and the first molecular dynamics stage that has to run. The following nine stages run in a sequential manner. Each stage generates a final configuration file, a trajectory of co-ordinates, a trajectory of energies, and an output of the molecular dynamics operation.

# Bibliography

- [1] L. S. B. University, url = <http://www1.lsbu.ac.uk/water/hyalgh.html> (2015).
- [2] L. Perić-Hassler and P. H. Hünenberger, *Interaction of alginate single-chain polyguluronate segments with mono- and divalent metal cations: a comparative molecular dynamics study*, Molecular Simulation **36**, 778 (2010).
- [3] M. D. Hanwell, D. E. Curtis, D. C. Lonie, T. Vandermeersch, E. Zurek, and G. R. Hutchison, *Avogadro: an advanced semantic chemical editor, visualization, and analysis platform*, Journal of cheminformatics **4**, 17 (2012).
- [4] N. I. of Standards and Technology, (2013).
- [5] W. Humphrey, A. Dalke, and K. Schulten, *Vmd: visual molecular dynamics*, Journal of molecular graphics **14**, 33 (1996).
- [6] L. J. Siqueira and M. C. Ribeiro, *Molecular dynamics simulation of the polymer electrolyte poly(ethylene oxide)/LiClO<sub>4</sub>. ii. dynamical properties*, The Journal of chemical physics **125**, 214903 (2006).
- [7] Y. Nishi, *Lithium ion secondary batteries; past 10 years and the future*, Journal of Power Sources **100**, 101 (2001).
- [8] M. Armand and J.-M. Tarascon, *Building better batteries*, nature **451**, 652 (2008).
- [9] S. S. Zhang, *Liquid electrolyte lithium/sulfur battery: Fundamental chemistry, problems, and solutions*, Journal of Power Sources **231**, 153 (2013).
- [10] D. Aurbach, Y. Talyosef, B. Markovsky, E. Markevich, E. Zinigrad, L. Asraf, J. S. Gnanaraj, and H.-J. Kim, *Design of electrolyte solutions for Li and Li-ion batteries: a review*, Electrochimica Acta **50**, 247 (2004).
- [11] K. Takada, *Progress and prospective of solid-state lithium batteries*, Acta Materialia **61**, 759 (2013).
- [12] J. C. Bachman, S. Muy, A. Grimaud, H.-H. Chang, N. Pour, S. F. Lux, O. Paschos, F. Maglia, S. Lupart, P. Lamp, et al., *Inorganic solid-state electrolytes for lithium batteries: mechanisms and properties governing ion conduction*, Chemical reviews **116**, 140 (2015).
- [13] Y. Zhao and L. L. Daemen, *Superionic conductivity in lithium-rich anti-perovskites*, Journal of the American Chemical Society **134**, 15042 (2012).
- [14] L. Long, S. Wang, M. Xiao, and Y. Meng, *Polymer electrolytes for lithium polymer batteries*, Journal of Materials Chemistry A **4**, 10038 (2016).
- [15] H. Zhang, P. Zhang, Z. Li, M. Sun, Y. Wu, and H. Wu, *A novel sandwiched membrane as polymer electrolyte for lithium ion battery*, Electrochemistry communications **9**, 1700 (2007).
- [16] A. Arya and A. Sharma, *Polymer electrolytes for lithium ion batteries: a critical study*, Ionics **23**, 497 (2017).
- [17] I. Kovalenko, B. Zdyrko, A. Magasinski, B. Hertzberg, Z. Milicev, R. Burtovyy, I. Luzinov, and G. Yushin, *A major constituent of brown algae for use in high-capacity Li-ion batteries*, Science , 1209150 (2011).



- [18] K. Soeda, Y. Matsui, M. Yamagata, and M. Ishikawa, *Application of alginate binders to graphite electrodes and characterization of their lithium-ion battery performance*, ECS Transactions **53**, 93 (2013).
- [19] S.-J. Zhang, Y.-P. Deng, Q.-H. Wu, Y. Zhou, J.-T. Li, Z.-Y. Wu, Z.-W. Yin, Y.-Q. Lu, C.-H. Shen, L. Huang, *et al.*, *Sodium-alginate-based binders for lithium-rich cathode materials in lithium-ion batteries to suppress voltage and capacity fading*, ChemElectroChem **5**, 1321 (2018).
- [20] D. Rees and J. Samuel, *The structure of alginic acid. part vi. minor features and structural variations*, Journal of the Chemical Society C: Organic, 2295 (1967).
- [21] Y. Yuguchi, H. Urakawa, K. Kajiwara, K. Draget, and B. Stokke, *Small-angle x-ray scattering and rheological characterization of alginate gels. 2. time-resolved studies on ionotropic gels*, Journal of Molecular Structure **554**, 21 (2000).
- [22] G. T. Grant, E. R. Morris, D. A. Rees, P. J. Smith, and D. Thom, *Biological interactions between polysaccharides and divalent cations: the egg-box model*, FEBS letters **32**, 195 (1973).
- [23] M. E. Tuckerman and G. J. Martyna, *Understanding modern molecular dynamics: Techniques and applications*, The Journal of Physical Chemistry B **105**, 7598 (2001).
- [24] S. Mogurampelly, O. Borodin, and V. Ganesan, *Computer simulations of ion transport in polymer electrolyte membranes*, Annual review of chemical and biomolecular engineering **7**, 349 (2016).
- [25] V. A. Payne, M. C. Lonergan, M. Forsyth, M. A. Ratner, D. F. Shriver, S. W. de Leeuw, and J. W. Perram, *Simulations of structure and transport in polymer electrolytes*, Solid state ionics **81**, 171 (1995).
- [26] L. Xie and G. Farrington, *Molecular mechanics and dynamics simulation of poly (ethylene oxide) electrolytes*, Solid State Ionics **53**, 1054 (1992).
- [27] F. Müller-Plathe and W. F. van Gunsteren, *Computer simulation of a polymer electrolyte: lithium iodide in amorphous poly (ethylene oxide)*, The Journal of chemical physics **103**, 4745 (1995).
- [28] A. Maitra and A. Heuer, *Cation transport in polymer electrolytes: A microscopic approach*, Physical review letters **98**, 227802 (2007).
- [29] O. Borodin and G. Smith, *Li+ transport mechanism in oligo (ethylene oxide) s compared to carbonates*, Journal of solution chemistry **36**, 803 (2007).
- [30] B. R. Brooks, C. L. Brooks III, A. D. Mackerell Jr, L. Nilsson, R. J. Petrella, B. Roux, Y. Won, G. Archontis, C. Bartels, S. Boresch, *et al.*, *Charmm: the biomolecular simulation program*, Journal of computational chemistry **30**, 1545 (2009).
- [31] W. R. Scott, P. H. Hünenberger, I. G. Tironi, A. E. Mark, S. R. Billeter, J. Fennen, A. E. Torda, T. Huber, P. Krüger, and W. F. van Gunsteren, *The gromos biomolecular simulation program package*, The Journal of Physical Chemistry A **103**, 3596 (1999).
- [32] D. A. Pearlman, D. A. Case, J. W. Caldwell, W. S. Ross, T. E. Cheatham III, S. DeBolt, D. Ferguson, G. Seibel, and P. Kollman, *Amber, a package of computer programs for applying molecular mechanics, normal mode analysis, molecular dynamics and free energy calculations to simulate the structural and energetic properties of molecules*, Computer Physics Communications **91**, 1 (1995).
- [33] D. Van Der Spoel, E. Lindahl, B. Hess, G. Groenhof, A. E. Mark, and H. J. Berendsen, *Gromacs: fast, flexible, and free*, Journal of computational chemistry **26**, 1701 (2005).
- [34] V. L. Larwood, B. J. Howlin, and G. A. Webb, *Solvation effects on the conformational behaviour of gellan and calcium ion binding to gellan double helices*, Molecular modeling annual **2**, 175 (1996).
- [35] W. of Chemicals, url = <http://www.worldofchemicals.com/chemicals/chemical-properties/alginic-acid.html> (2018).

- [36] R. W. Hockney, *The potential calculation and some applications*, Methods Comput. Phys. **9**, 136 (1970).
- [37] J.-P. Ryckaert, G. Ciccotti, and H. J. Berendsen, *Numerical integration of the cartesian equations of motion of a system with constraints: molecular dynamics of n-alkanes*, Journal of Computational Physics **23**, 327 (1977).
- [38] H. J. Berendsen, J. v. Postma, W. F. van Gunsteren, A. DiNola, and J. Haak, *Molecular dynamics with coupling to an external bath*, The Journal of chemical physics **81**, 3684 (1984).
- [39] W. F. van Gunsteren and H. J. Berendsen, *Computer simulation of molecular dynamics: Methodology, applications, and perspectives in chemistry*, Angewandte Chemie International Edition in English **29**, 992 (1990).
- [40] W. F. van Gunsteren, S. R. Billeter, A. A. Eising, P. H. Hünenberger, P. Krüger, A. E. Mark, W. R. Scott, and I. G. Tironi, *Biomolecular simulation: the {GROMOS96} manual and user guide*, (1996).
- [41] A. P. Eichenberger, J. R. Allison, J. Dolenc, D. P. Geerke, B. A. Horta, K. Meier, C. Oostenbrink, N. Schmid, D. Steiner, D. Wang, *et al.*, *Gromos++ software for the analysis of biomolecular simulation trajectories*, Journal of chemical theory and computation **7**, 3379 (2011).
- [42] T. Cottrell, *The strengths of chemical bonds*, 2nd edn, butterwoth, london, 1958 search pubmed;(b) b. deb. darwent, national standard reference data series, national bureau of standards, no. 31, washington, 1970 search pubmed;(c) sw benson, J. Chem. Educ **42**, 502 (1965).